HOKKAIDO UNIVERSITY

Title	Structural Insights into Autophagy in the AlphaFold Era
Author(s)	Maruyama, Tatsuro; Noda, Nobuo N.
Citation	Journal of Molecular Biology, 437(18), 169235 https://doi.org/10.1016/j.jmb.2025.169235
Issue Date	2025-09-15
Doc URL	https://hdl.handle.net/2115/98004
Rights	© 2025. This manuscript version is made available under the CC-BY-NC-ND 4.0 license https://creativecommons.org/licenses/by-nc-nd/4.0/
Rights(URL)	https://creativecommons.org/licenses/by-nc-nd/4.0/
Type	journal article
File Information	JMB-revise-final.pdf

Hokkaido University Collection of Scholarly and Academic Papers : HUSCAP

Structural insights into autophagy in the AlphaFold era

Tatsuro Maruyama[1] and Nobuo N. Noda[1,2]
1- Institute of Microbial Chemistry (BIKAKEN), Tokyo 141-0021, Japan.
2- Institute for Genetic Medicine, Hokkaido University, Sapporo 060-0815, Japan.
Correspondence to Tatsuro Maruyama: Institute of Microbial Chemistry (BIKAKEN), 3-14-23 Kamiosaki, Shinagawa-ku, Tokyo 141-0021, Japan. maruyamat@bikaken.or.jp; Nobuo N. Noda: Institute for Genetic Medicine, Hokkaido University, Kita 15, Nishi 7, Kita-ku, Sapporo 060-0815, Japan. nn@igm.hokudai.ac.jp

Abstract
Autophagy, a lysosomal intracellular degradation system, is characterized by the de novo biogenesis of autophagosomes. This biogenesis is mediated by approximately 20 core Atg proteins, exhibiting a high degree of conservation from yeast to humans. Over the preceding two decades, the structural biology of autophagy has been investigated predominantly through X-ray crystallography, NMR spectroscopy, and, more recently, cryo-electron microscopy, collectively contributing to the elucidation of the structural basis of core Atg proteins. The recent introduction of AlphaFold has significantly improved the precision of structure prediction and is transforming structural biology research. In this review, we aim to synthesize the structural basis of the operational mechanisms of the core Atg proteins, employing structures predicted by AlphaFold, and to discuss the molecular mechanisms that drive autophagosome biogenesis.

Key words: AlphaFold, AlphaFold2, AlphaFold3, autophagosome formation, autophagy

Abbreviations: 17BR, Atg17-binding region; 17LR, Atg17-linking region; AH, amphipathic helix; BARA, beta-alpha repeated, autophagy-specific; BATS, Barkor/Atg14(L) autophagosome targeting sequence; CC, coiled-coil; Cryo-EM, cryo-electron microscopy; CTD, C-terminal domain; ER, endoplasmic reticulum; FR, flexible region; HR, handle region; IDR, intrinsically disordered region; IM, isolation membrane; MIM, MIT-interacting motif; NHD, N-terminal helical domain; NTD, N-terminal domain; PAS, pre-autophagosomal structure; PE, phosphatidylethanolamine; PI, phosphatidylinositol; PI3KC3-C1, Class III phosphatidylinositol 3-kinase complex 1; PI3P, phosphatidylinositol 3-phosphate; tMIT, tandem microtubule-interacting and transport domain; ULD, ubiquitin-like domain.

Introduction

Autophagy, a key cellular process for degradation, is defined by the biogenesis of autophagosomes [1]. Around 20 core Atg factors are essential for this biogenesis, working in six functional groups: i) the autophagy-initiating Atg1/ULK complex; ii) the autophagy-specific Class III phosphatidylinositol (PI) 3-kinase complex 1 (PI3KC3-C1); iii) the lipid scramblase Atg9; iv) the lipid transfer Atg2–Atg18 complex; v) the Atg12–Atg5 conjugation system; and vi) the Atg8 lipidation system (Figure 1) [1, 2]. Structural investigations of these core Atg factors have been primarily carried out over the past two decades using X-ray crystallography, NMR spectroscopy, and more recently cryo-electron microscopy (Cryo-EM), establishing most of their three-dimensional structures and some of their interactions [3, 4]. The recent introduction of AlphaFold has dramatically increased the accuracy of structure prediction, now allowing relatively straightforward prediction of structures for individual proteins and even complexes, and is starting to revolutionize life science [5-7]. This review provides a summary of the structural basis of the functional mechanisms of the core Atg factors essential for autophagosome formation, drawing upon structures predicted by AlphaFold3 and, where more appropriate, AlphaFold2. We have primarily focused on AlphaFold predictions that are congruent with prior experimentally resolved structures and mutational data, but have also included predictions awaiting experimental validation. We hope this review will serve as a valuable resource to advance autophagy research in the transformative AlphaFold era. For a detailed review of the structural analysis of core Atg factors using experimental techniques, we refer you to our recent review articles [3, 4].

Main

The Atg1/ULK complex in autophagy initiation

The Atg1 complex, responsible for initiating autophagy in budding yeast (Figure 1) [8], is composed of a protein kinase Atg1, an intrinsically disordered protein Atg13, and a scaffolding subcomplex of Atg17–Atg29–Atg31. The mammalian equivalent, known as the ULK complex, includes ULK1 or ULK2 (homologs of Atg1), ATG13, FIP200/RB1CC1 (functionally analogous to Atg17), and ATG101 [9].

The Atg1 complex

The Atg1 complex is organized centrally by Atg13, which contains a globular Hop1, Rev7, Mad2 (HORMA) domain and an intrinsically disordered region (IDR) (Figure 2A). This IDR is critical for its interaction with Atg1 and Atg17 [10-13]. Atg1 itself features an N-terminal kinase domain and a C-terminal tandem microtubule-interacting and trafficking (tMIT) domain, linked by an IDR (Figure 2B) [11, 12]. A key interaction occurs between the tMIT domain of Atg1 and two MIT-interacting motifs (MIMs) located within the IDR of Atg13 (Figure 2B) [11]. In contrast to the dynamic nature of

these components, the Atg17–Atg29–Atg31 complex forms a stable unit: Atg17, largely α-helical, forms an S-shaped homodimer, providing a concave surface for the attachment of the Atg29–Atg31 subcomplex (Figure 2C) [14]. An IDR is uniquely present at the C-terminus of Atg29 [15]. Within the Atg13 IDR are at least two binding elements, the Atg17-binding region (17BR) and the Atg17-linking region (17LR), which target distinct regions on Atg17 (Figure 2C) [13]. Critically, the AlphaFold model (Figure 2C) highlights that distance limitations prevent 17BR and 17LR from a single Atg13 molecule simultaneously engaging a single Atg17 dimer. As a result, Atg13 bridges two separate Atg17 dimers using 17BR and 17LR, initiating the higher-order assembly of the Atg1 complex (Figure 2D) [13] and driving its liquid-liquid phase separation (Figure 2E) [16]. These Atg1 complex condensates then organize the pre-autophagosomal structure (PAS) in yeast, a key site where autophagosome formation is facilitated by concentrating Atg factors like the Atg12–Atg5–Atg16 complex and precursor Atg9 vesicles, and by promoting crucial enzymatic reactions for autophagy (Figure 2E) [16, 17]. The Atg13 IDR contains numerous serine and threonine residues whose phosphorylation status is regulated by kinases and phosphatases; phosphorylation at 17BR and MIM has been shown to disrupt the formation of the Atg1 complex and PAS assembly, thereby inhibiting the initiation of autophagy (Figure 2D) [11, 16, 18].

The ULK complex

Although sharing HORMA and IDR features with yeast Atg13, mammalian ATG13 uniquely forms a stable complex with ATG101, another HORMA protein present in fission but not budding yeast (Figure 3A) [19-24]. The binding of this ATG13–ATG101 HORMA pair to ATG9A requires a conformational change in the HORMA folds [25, 26]. ULK1 and ULK2, homologs of yeast Atg1 (Figure 3B) [27, 28], consists of an N-terminal kinase domain, a C-terminal tMIT, and an intervening IDR, and they interact with the MIMs of ATG13. In contrast, while the N-terminal domain (NTD) of the large 1594-amino acid protein FIP200 shows weak homology to the NTD of the smaller 417-amino acid Atg17, their homodimeric structures differ: FIP200 NTD forms a U-shape (Figure 3C) [29], whereas Atg17 forms an S-shape. FIP200 also possesses a C-terminal Claw domain (named for its characteristic shape) that interacts with selective autophagy receptors and the NTD, with these regions linked by an exceptionally long α-helix forming a parallel coiled-coil (CC) in the dimeric assembly (Figure 3C) [30, 31].

A key strength of the AlphaFold prediction is the atomic visualization it offers of the extended FIP200 structure. In contrast to yeast Atg13 IDR binding two separate Atg17 dimers, mammalian ATG13 binds two NTDs within a single FIP200 NTD dimer, a structural distinction clearly revealed by AlphaFold (Figure 3D) [27-29]. Additionally, ULK1 tMIT directly binds the FIP200 NTD, forming a tripartite complex with FIP200 and ATG13 (Figure 3D) [27, 28]. This single FIP200 dimer binding by ATG13 prevents it from driving higher-order ULK complex assembly in the same way yeast Atg13 assembles

the Atg1 complex. Nevertheless, FIP200 and ATG13 have been shown to undergo phase separation to organize a mammalian autophagosome formation site through mechanisms that remain unclear [32]. Recent findings indicate that the interaction between the ULK complex and PI3KC3-C1 allows two ATG13 molecules to interact with an FIP200 dimer, potentially providing a mechanistic basis for the observed phase separation of the ULK complex [27].

The autophagy-specific phosphatidylinositol 3-kinase complex

In budding yeast, PI3KC3-C1 consists of the catalytic subunit Vps34 and the accessory proteins Vps15, Atg14, Atg6/Vps30, and Atg38; the mammalian equivalent shares this composition, with Atg6 named Beclin 1 and Atg38 NRBF2 (Figure 1) [33-36]. The V-shaped overall structure of PI3KC3-C1 features one arm composed of the helical and kinase domains of Vps34 and Vps15, and the other arm formed by the Atg6/Beclin 1-Atg14 heterodimer along with the WD40 domain of Vps15 (Figure 4) [37-39]. Functionally, the beta-alpha repeated, autophagy-specific (BARA) domain of Atg6/Beclin 1, with its aromatic finger, and the Barkor/Atg14 autophagosome targeting (BATS) motif of Atg14, both located at one end of the V's arms, are known to interact with membranes [40-42]. Conversely, the kinase domain of Vps34 resides at the other end (Figure 4). This spatial arrangement strongly implies that PI3KC3-C1 binds to the membrane via these two ends, positioning the Vps34 kinase domain to catalyze PI phosphorylation, as illustrated in Figure 4.

As previously described, the structure of the PI3KC3-C1 complex exhibits similarity between yeast and mammals; however, the mode of interaction of the fifth component, yeast Atg38, and mammalian NRBF2, demonstrates divergence. Both Atg38 and NRBF2 are characterized by an N-terminal MIT domain and a C-terminal CC domain responsible for homodimerization (Figure 4). The MIT domains of both proteins exhibit a similar binding affinity for Vps15 and the BH3 domain of Atg6/Beclin 1 (Figure 4). Remarkably, the MIT domain of Atg38 also binds to Atg14, facilitating the binding of one Atg38 homodimer to a single PI3KC3-C1 complex and contributing to its structural integrity (Figure 4A) [34]. Conversely, convergent prediction by AlphaFold did not identify a second binding site for the MIT domain of NRBF2 within the human PI3KC3-C1 complex. Consistent with this, it has been proposed that one NRBF2 homodimer interacts with two PI3KC3-C1 complexes, thereby promoting their dimerization (Figure 4B) [43, 44]. However, biochemical and structural investigations have posited the existence of a second, minor binding site for the MIT domain of NRBF2 within human PI3KC3-C1. The binding of a single NRBF2 homodimer to both the major and minor binding sites of a single PI3KC3-C1 complex has been proposed to activate its kinase activity through modulation of the kinase domain's conformation [45]. Further investigation is warranted to more comprehensively delineate the conserved and divergent roles of NRBF2 and Atg38 in the regulation of PI3KC3-C1 activity. The recruitment of PI3KC3-C1 to the autophagosome formation site in yeast is contingent upon the interaction between the IDR of Atg29 and the CC domain of Atg38 (a prediction derived

from AlphaFold lacking experimental structural validation) and the interactions between the BARA domain of Atg6 and the IDR of Atg9 [46]. Upon recruitment, PI3KC3-C1 generates PI-3 phosphate (PI3P) at autophagic membranes, which plays pivotal roles in the recruitment of PROPPIN (β-propellers that bind polyphosphoinositides) family proteins, as described subsequently [47, 48].

The lipid scrambling function of Atg9 and the lipid-transferring activity of the Atg2–Atg18 complex

The biogenesis of a single autophagosome necessitates the incorporation of millions of lipid molecules, which are considered to be predominantly sourced from the endoplasmic reticulum (ER) [1]. Atg9 and the Atg2–Atg18 complex represent the principal factors involved in lipid supply, and the mechanisms governing their operation have only recently begun to be elucidated [49, 50].

Atg9

Atg9 represents the sole transmembrane protein within the complement of core Atg proteins [1]. In yeast, Atg9 is integrated into vesicles designated Atg9 vesicles at the Golgi apparatus, and these vesicles are dispersed throughout the cytoplasm under nutrient-replete conditions [51]. Upon the induction of starvation, a subset of Atg9 vesicles targets PAS in yeast and is proposed to serve as the initial membrane source for the generation of isolation membranes (IMs), also known as phagophores, wherein Atg9 is incorporated and localized at the expanding margin of the IM [51-53]. ATG9A, the mammalian orthologue of yeast Atg9, similarly exists in vesicular form. While it has been previously posited that ATG9A transiently associates with the site of autophagosome formation before immediate dissociation without incorporation into the IM [54-56], recent reports suggest that a minor fraction of ATG9A is indeed incorporated into the IM, analogous to the behavior observed for yeast Atg9 [57, 58]. Atg9-family proteins are structurally defined by four transmembrane helices, two laterally-membrane-buried helices, and long IDRs at both ends that enable interaction with other Atg proteins like Atg13 (Figure 5A) [25, 59-62]. These proteins assemble as homotrimers, forming a vertical pore at the trimer's center spanning the membrane and a lateral pore within each protomer, with these pores being interconnected [59-61]. While the molecular function of Atg9 remained a long-standing mystery since its discovery, recent functional assays using purified proteins have revealed that both yeast Atg9 and human ATG9A exhibit lipid scrambling activity, likely utilizing the described vertical and lateral pores (Figure 5A) [60, 61, 63]. This scrambling activity is proposed to allow Atg9-family proteins to distribute phospholipids, delivered from the ER by the Atg2–Atg18 complex, to both sides of the IM, thus promoting its growth [49, 60, 61, 64].

The Atg2–Atg18 complex

Atg2 forms a stable complex with Atg18, a protein belonging to the PROPPIN family, and its

localization to the expanding margin of the IM is mediated through interactions with PI3P and Atg9 [47, 52]. Additionally, the N-terminal region of Atg2 interacts with the ER, especially ER exit sites, effectively tethering the ER to the IM via the Atg2–Atg18 complex [65-67]. The primary function of Atg2, its ability to transfer lipids between membranes, has recently been clarified for both yeast Atg2 and human ATG2A/2B [68-71]. Figure 5B illustrates the structures of the yeast Atg2–Atg18 complex (top) and the human ATG2A–WIPI4 (an Atg18 homolog) complex (bottom). Both Atg2 and ATG2A exhibit a rod-like architecture with a central, elongated hydrophobic cavity [72-75]. Atg18 and WIPI4 bind to the C-terminal side of their respective Atg2/ATG2A partners. While Cryo-EM has recently provided structures of ATG2A and the ATG2A–WIPI4 complex, AlphaFold offers a key advantage by predicting atomic models that include the membrane binding terminal regions of ATG2A and the complete interaction interface of the ATG2A–WIPI4 complex, details that were not resolved by Cryo-EM. Furthermore, Atg2/ATG2A possesses a Chorein_N domain with weak sequence similarity to Vps13 family proteins, another group known to have lipid transfer activity [76]. The proposed mechanism for IM expansion in yeast involves the Atg2–Atg18 complex bridging the ER and the growing edge of the IM: the N-terminus of Atg2 interacts with the ER, while the C-terminus of Atg2 and Atg18 interact with the IM, facilitating the transfer of lipids from the ER to the IM (Figure 5B) [69, 77]. A comparable mechanism is thought to operate for the mammalian ATG2A/2B–WIPI complex [68, 70, 71]. Because Atg2 is not a transmembrane protein and transfers lipids only to the cytosolic leaflet of the IM, lipids delivered to the cytosolic leaflet of the IM by Atg2 must be transported to the luminal leaflet of the IM for membrane expansion. As described above, Atg9 is proposed to mediate this function [49, 60, 61]. Although Cryo-EM has shown interactions between ATG2A and ATG9A [72, 73], the exact nature of these interactions is still debated, with several models proposed, none of which have been predicted by AlphaFold. Further research is needed to clarify the functionally important interactions in autophagy. Given the structural potential of Atg2 for bidirectional lipid transport, external factors that ensure unidirectional movement from the ER to the IM are crucial for IM expansion, one being the new synthesis of phospholipids at the ER [78, 79].

Systems for Atg12–Atg5 conjugation and Atg8 lipidation

For the expansion of the IM during autophagosome formation, the Atg12–Atg5 conjugation and Atg8 lipidation systems are indispensable [80-83]. Atg12 and Atg8 are both ubiquitin-like proteins that are conjugated through ubiquitylation-like reactions, a process facilitated by autophagic E1, E2, and E3 enzymes (Figure 1). Remarkably, the Atg12−Atg5 conjugate acts as an E3 enzyme within the Atg8 lipidation system, mediating a distinctive conjugation between a protein and a phospholipid molecule. Due to the strong conservation of these systems across yeast and humans, our primary focus in this section will be on their structures, enzymatic reaction pathways, and membrane-associated functions as studied in yeast, with comparative references to their human counterparts.

The Atg12−Atg5 conjugation system

The Atg12–Atg5 conjugation system, depicted with purple arrows in Figure 6A, involves several key structural components. Atg12 (dark purple) features an N-terminal IDR and a ubiquitin-like domain (ULD) (Figure 6A) [84]. The E1 enzyme Atg7 (orange) possesses an NTD and a C-terminal domain (CTD) connected by a linker [85-87]. Dimerization of Atg7 occurs through its CTDs, which include an adenylation domain and a C-terminal IDR. The C-terminal glycine of Atg12 is activated by ATP-dependent adenylation, forming a thioester intermediate with Atg7, which then reacts with the catalytic site of the E2 enzyme, Atg10 (dark green) [88, 89]. Atg10, characterized by a canonical E2 core domain with an additional α helix and β sheet [90, 91], binds to the NTD of Atg7 (Figure 6A). The Atg12~Atg10 thioester intermediate forms *in trans* on the Atg7 dimer [88, 89]. The C-terminus of Atg12 is then covalently linked to a lysine residue of Atg5, a protein composed of two ULDs and a helix-rich domain [92-94]. Finally, Atg5 is stably bound to Atg16 (light purple), which contains an Atg5-binding region and a parallel CC domain (Figure 6A) [94-96]. The PROPPIN family protein Atg21 plays a role in regulating the E3 ligase complex by binding to the CC domain of Atg16, which facilitates the localization of the E3 to PI3P-rich autophagic membranes (Figure 6A, left bottom) [97-99]. Human cells express ATG16L1 and ATG16L2 as homologs of Atg16, with ATG16L1 being the more studied [100]. Structurally, ATG16L1 contains an ATG5-binding region, a parallel CC domain, an IDR, and a WD40 repeat domain, although this last domain is not required for autophagy (Figure 6B) [101]. The ATG12–ATG5–ATG16L1 complex shows a preference for binding to highly curved membranes via its N-terminal region [102, 103], and other regions within ATG16L1 also contribute to membrane binding [102, 104]. Moreover, the interaction of WIPI2, a homolog of yeast Atg18 and Atg21, with multiple sites on the ATG16L1 CC domain is crucial for proper E3 ligase activity (Figure 6B) [105-109]. The lack of experimentally resolved atomic structures for these complete E3 complexes and their interactions with PROPPINs underscores the utility of AlphaFold prediction. The autophagic E3 enzyme possesses a distinct overall structure compared to canonical E3 enzymes, with the Atg12–Atg5 conjugate serving as the E3 component within the Atg8 lipidation system [110, 111].

The Atg8 lipidation system

The Atg8 lipidation system, shown with blue arrows in Figure 6A, involves a single protein, Atg8, in yeast, but a family of six homologs—LC3A, LC3B, LC3C, GABARAP, GABALAPL1, and GABARAPL2—in humans (Figure 6A, cyan) [112]. Despite their individual roles in autophagy regulation, with LC3B and GABARAP being extensively studied, these homologs share similar structural features [112-115]. Atg8 itself is structurally defined by an N-terminal helical domain (NHD) and a ULD [116]. Remarkably, Atg8-family interacting motifs (AIMs) and LC3-interacting regions (LIRs), characterized by the consensus sequence (W/F/Y)xx(I/L/V) (where x can be any amino

acid), are prevalent in various proteins, including the core Atg machinery, and exhibit moderate binding strengths (Figure 6A, bottom right) [112, 117-121].

Newly synthesized Atg8 must first be processed by the cysteine protease Atg4 to expose its C-terminal glycine residue [122]. Atg4 (yellow, Figure 6A) possesses a papain-like protease domain, a short-fingers domain, and IDRs at both its N- and C-termini [123-125]. This processing involves recognition of Atg8 by the short-fingers domain and an AIM motif in the C-terminal IDR of Atg4, ensuring accurate cleavage [123, 126]. In humans, there are four ATG4 isoforms (ATG4A, ATG4B, ATG4C, and ATG4D) with unique substrate specificities and activities [127]. Similar to Atg12, the processed Atg8 is then adenylated in an ATP-dependent manner by the E1 enzyme Atg7, forming an Atg8~Atg7 thioester intermediate (Figure 6A, center) [85-87]. However, unlike Atg12, Atg8 subsequently forms a thioester intermediate with the E2 enzyme, Atg3 (light green), which contains an N-terminal amphipathic helix (AH), a flexible region (FR), and a handle region (HR) in addition to a canonical E2 core domain [128]. Atg3 interacts with the NTD of Atg7 via its E2 core domain and FR, facilitating the formation of a thioester intermediate with Atg8 in a *trans* configuration on the Atg7 dimer [85, 86]. Subsequently, the FR of Atg3 engages with the Atg12 moiety of the E3 enzyme, inducing a conformational change in the catalytic site of Atg3, which facilitates the transfer of Atg8 to phosphatidylethanolamine (PE) phospholipids [129-132]. Furthermore, the N-terminal AH within Atg3 recognizes membrane packing defects, particularly those present in highly curved membranes, thereby promoting the transfer of Atg8 to PE within the autophagic membranes (Figure 6A, light green in the bottom) [133, 134]. The less bulky and hydrophobic nature of the human ATG3 AH allows for a more refined interaction with autophagic membranes [135]. The E3−PROPPIN complex further ensures correct localization and efficient Atg8–PE conjugation on autophagic membranes [99, 107, 109]. The resulting Atg8–PE conjugate exhibits membrane tethering, hemi- or full-fusion, and membrane perturbation activities, all likely contributing to autophagosome biogenesis, although their precise functions are still under investigation [83, 136-140].

Atg4 also functions to delipidate Atg8–PE by cleaving the amide bond linking Atg8 and the PE lipid, releasing free Atg8 [80, 123]. This delipidation activity by Atg4 primarily occurs on inappropriate membranes within the cell, allowing for the recycling of Atg8 for subsequent lipidation at the correct autophagic membranes [141-143]. Furthermore, the Atg1 kinase negatively regulates Atg8–PE levels on the IM by phosphorylating the E2 and E3 enzymes involved in its formation, thereby suppressing their activity [144]. Because the abundance of Atg8–PE is directly linked to autophagosome formation [82], and the accumulation of excessive Atg8–PE on the IM hinders its expansion [145], the formation of Atg8–PE is precisely controlled in both space and time through the coordinated actions of core Atg proteins, utilizing their unique structural architectures to ensure proper autophagosome biogenesis.

In addition to its role in protein-phospholipid conjugation, the Atg8 lipidation system is critical for the structural formation of a dynamic membrane scaffold (Figure 6C) [146-148]. Evidence from *in*

vitro reconstitution studies indicates that these enzymes associate with Atg8–PE through multiple interactions involving their IDRs (Figure 6C), resulting in a flexible, meshwork-like scaffold on the membrane. This scaffold's ability to induce membrane remodeling is analogous to the observed transition from sheet-like to cup-like IM structures during autophagosome formation. Therefore, beyond their enzymatic functions, the E1, E2, and E3 enzymes of the Atg8 lipidation system utilize their unique structural architectures to build an autophagic membrane scaffold with Atg8–PE, effectively driving the membrane remodeling necessary for autophagosome formation.

Using AlphaFold in autophagy research

The majority of the information presented thus far has been derived from insights gained through experimental structural analysis methodologies. AlphaFold possesses an astonishing capability: it can predict the structures of all Atg proteins within a matter of hours, a process that has required over two decades to elucidate experimentally. Beyond its speed, a significant advantage lies in its capacity to predict the architectures of large or highly flexible proteins. For example, AlphaFold models of the Atg1/ULK complex, which contains elongated CC domains and extensive IDRs, aid in clarifying their overall shapes and offer insights into how these proteins organize higher-order scaffolding, a process crucial for autophagosome assembly. Such rapid structure determination also facilitates the design of targeted mutational studies aimed at validating predicted interaction interfaces, thereby accelerating the generation of testable hypotheses. A further benefit of AlphaFold lies in its utility in illuminating previously elusive protein-protein interactions. Within the ULK complex, AlphaFold predictions have revealed the interaction between the IDR of ATG13 and the N-terminal domain of FIP200. Similar advancements have been achieved in understanding the PI3KC3-C1 complex, particularly concerning the binding of Atg38 to other subunits and to Atg29. AlphaFold also provides a valuable complement to high-resolution techniques, including Cryo-EM. Although Cryo-EM has provided groundbreaking insights into large complexes like the ATG2A–WIPI4 complex, the dynamic nature of terminal regions often limits their structural resolution. By synergistically combining experimental Cryo-EM data with AlphaFold-generated models, researchers can gain a more complete picture of how ATG2A utilizes its terminal regions to interact with the ER and IM during autophagosomal membrane expansion. Importantly, computational structure prediction is also paving the way for new therapeutic strategies. With autophagy dysregulation being implicated in a range of diseases, including neurodegeneration and cancer, AlphaFold models offer a powerful platform for rational drug design, potentially enabling the identification of small molecules or peptides that can selectively modulate autophagy. Therefore, AlphaFold not only significantly accelerates fundamental discoveries in autophagy research but also holds substantial promise for driving clinical applications.

Concluding remarks

The structural basis of autophagosome biogenesis has significantly advanced our knowledge of autophagy. While X-ray crystallography, NMR spectroscopy, and Cryo-EM have provided valuable atomic models for many Atg proteins and complexes, AlphaFold-based structure predictions are rapidly yielding insights into complex multimeric assemblies and protein-protein interfaces that have so far eluded experimental determination. Remarkably, predictions that are consistent with mutational and biochemical findings can illuminate previously unrecognized interactions or direct targeted experiments to confirm their functional importance. Despite the increasing clarity surrounding the molecular mechanisms of autophagosome formation, significant questions remain, including the precise mechanisms regulating lipid transfer and the interplay between phase-separated autophagy complexes and membrane remodeling events. The continued synergistic integration of powerful computational approaches like AlphaFold with biochemical and biophysical experiments promises to significantly further our understanding of autophagy, leading to new discoveries in this dynamic and crucial field.

Acknowledgments

We thank ChatGPT (OpenAI) for providing language editing assistance on an early draft of this manuscript. This work was supported in part by JSPS KAKENHI JP24K09373 (to T.M.), JP23K20044, JP24H00060, JP25H00966, JP25H01320, and JP25H01321 (to N.N.N.), CREST, Japan Science and Technology Agency Grant number JPMJCR20E3 (to N.N.N.), and grants from the Takeda Science Foundation (to T.M., N.N.N.).

Figure legends

Figure 1. Summary of the core Atg proteins responsible for autophagosome formation.
Autophagosome formation in yeast is initiated by the Atg1 complex (Atg1, Atg13, Atg17, Atg29, Atg31), which organizes the PAS. The PAS then recruits the Atg9-containing vesicles, providing the initial membrane source, and the PI3KC3-C1 complex (Atg6, Atg14, Atg38, Vps15, Vps34), which generates the signaling lipid PI3P on these vesicles. This PI3P then serves as a docking site for the Atg2–Atg18 complex and Atg21. The Atg2–Atg18 complex acts as a tether between the ER and the nascent autophagic membranes, facilitating lipid transfer from the ER, a process aided by the lipid scramblase activity of Atg9. Atg21 then recruits the Atg12–Atg5–Atg16 complex, a product of Atg7- and Atg10-dependent conjugation. Finally, this complex, along with Atg4, Atg7, and Atg3, mediates the reversible generation of Atg8–PE on autophagic membranes, leading to the formation of the autophagic membrane scaffold on the IM and the progression of autophagosome formation. The corresponding human Atg complexes are listed at the bottom.

Figure 2. Structural insights into the yeast autophagy initiation complex.
(A–C) AlphaFold-predicted structures of (A) Atg13, (B) the Atg1–Atg13 MIM complex, and (C) the Atg17–Atg29–Atg31–Atg13 (17BR/17LR) complex, highlighting that Atg13 (17BR/17LR) segments do not form intramolecular crosslinks within an Atg17 dimer, as shown in (C).
(D) Regulation of Atg1 complex formation through phosphorylation of Atg13.
(E) Schematic representation illustrating how the IDRs of Atg13 (depicted as lines) bridge separate Atg17–Atg29–Atg31 dimers via the 17BR and 17LR segments to drive liquid-liquid phase separation of the Atg1 complex, leading to PAS recruitment of downstream Atg factors that directly interact with the Atg1 complex. The structures presented in this manuscript were generated using AlphaFold3 predictions unless otherwise specified and visualized with ChimeraX [149].

Figure 3. Structural analysis of the human autophagy initiation complex.
(A–D) AlphaFold-predicted structures of (A) the ATG13–ATG101 complex, (B) ULK1–ATG13 MIM, and (C) FIP200. The bottom panels in (A) provide a comparative view of the yeast Atg13 HORMA domain (left) and the human ATG13 HORMA–ATG101 complex (right), highlighting evolutionary conservation. Similarly, the bottom panels in (B) compare the yeast Atg1 tMIT–Atg13 MIM interaction (left) with the corresponding human ULK1 tMIT–ATG13 MIM interaction (right). Given the predicted high structural similarity to ULK1, the ULK2 structure is not presented. (D) Schematic representation of the mammalian ULK1 complex assembly, informed by AlphaFold predictions. The structural model of the FIP200 NTD in complex with the ATG13 IDR and ULK1 tMIT was generated using AlphaFold2 predictions. IDRs are represented as lines. For clarity, the CC and Claw domains of FIP200 have been omitted.

Figure 4. Structural insights into the PI3KC3-C1 complex.

(A,B) AlphaFold-predicted structures of the PI3KC3-C1 complex, illustrating the distinct subunit compositions in (A) yeast (Atg6, Atg14, Vps15, Vps34, Atg38) and (B) humans (BECN1 [Beclin 1], ATG14, VPS15, VPS34, NRBF2). The BARA and BATS domains are crucial for the interaction of both complexes with autophagic membranes. A key difference lies in the role of the MIT domains: in yeast, the two MIT domains from an Atg38 homodimer bind to separate subcomplexes (Vps15–Vps34 and Atg6–Atg14) to stabilize PI3KC3-C1, whereas in humans, the two MIT domains from an NRBF2 homodimer bind to two VPS15 molecules, promoting dimerization of the entire complex. An alternative model suggests a regulatory role for the NRBF2 MIT domain, involving weak binding to another site within the same PI3KC3-C1 to potentially activate its kinase activity. The product of the kinase activity of VPS34, PI3P (represented with a circled P), serves as a key recruitment signal for PROPPIN proteins (Atg18 and Atg21 in yeast, and WIPIs in humans).

Figure 5. The lipid supply system in autophagy.

(A) AlphaFold-predicted structures of the lipid scramblase Atg9 (yeast) and its human counterpart ATG9A (IDRs shown as lines). Both proteins are localized to small cytoplasmic vesicles and exhibit lipid scramblase activity. A key difference lies in their interaction partners: the IDRs of yeast Atg9 interact with Atg6 and Atg13, while the IDRs of human ATG9A interact with the ATG13-ATG101 complex.

(B) AlphaFold-predicted structures of the lipid transfer complexes Atg2–Atg18 (yeast) and ATG2A–WIPI4 (human). The Chorein_N domain mediates binding to the ER in both systems, while Atg18 (yeast) and WIPI4 (human) bind PI3P enriched at the IM, thus connecting the ER to the IM. Both Atg2 and ATG2A facilitate direct lipid transfer from the ER to the IM via elongated hydrophobic channels, crucial for IM expansion.

Figure 6. The Atg12–Atg5 conjugation and Atg8 lipidation systems.

(A) An overview of the Atg12–Atg5 conjugation and Atg8 lipidation systems, informed by AlphaFold-predicted structures. In humans, the LC3 and GABARAP families are the functional equivalents of yeast Atg8. The pathways for the Atg12–Atg5 conjugation and Atg8 lipidation are depicted by purple and blue arrows, respectively. The PROPPIN family member Atg21, by interacting with both the E3 ligase and PI3P on autophagic membranes, defines the site of Atg8–PE production. The AH of Atg3 interacts with autophagic membranes, facilitating the transfer of Atg8 from Atg3 to PE. Once formed on autophagic membranes, Atg8–PE interacts with various proteins, including Atg1, Atg3, Atg4, and Atg7, through their AIM/LIR motifs.

(B) AlphaFold-predicted structure of the human E3 ligase complex ATG12–ATG5–ATG16L1–

WIPI2. Both Atg21 and WIPI2, belonging to the PROPPIN family, bind PI3P on autophagic membranes, a crucial step for proper localization of the conjugation machinery.
(C) Summary of the interactions between the components of the Atg8 conjugation machinery that are essential for building the autophagic membrane scaffold.

[1] Nakatogawa, H. (2020). Mechanisms governing autophagosome biogenesis. Nat. Rev. Mol. Cell Biol. **21**, 439-458. https://doi.org/10.1038/s41580-020-0241-0.

[2] Noda, N. N. & Inagaki, F. (2015). Mechanisms of Autophagy. Annu Rev Biophys. **44**, 101-122. https://doi.org/10.1146/annurev-biophys-060414-034248.

[3] Noda, N. N. (2024). Structural view on autophagosome formation. FEBS Lett. **598**, 84-106. https://doi.org/10.1002/1873-3468.14742.

[4] Matoba, K. & Noda, N. N. (2021). Structural catalog of core Atg proteins opens new era of autophagy research. J Biochem. **169**, 517-525. https://doi.org/10.1093/jb/mvab017.

[5] Abramson, J., Adler, J., Dunger, J., Evans, R., Green, T., Pritzel, A., Ronneberger, O., Willmore, L., Ballard, A. J., Bambrick, J., Bodenstein, S. W., Evans, D. A., Hung, C. C., O'Neill, M., Reiman, D., Tunyasuvunakool, K., Wu, Z., Žemgulytė, A., Arvaniti, E., Beattie, C., Bertolli, O., Bridgland, A., Cherepanov, A., Congreve, M., Cowen-Rivers, A. I., Cowie, A., Figurnov, M., Fuchs, F. B., Gladman, H., Jain, R., Khan, Y. A., Low, C. M. R., Perlin, K., Potapenko, A., Savy, P., Singh, S., Stecula, A., Thillaisundaram, A., Tong, C., Yakneen, S., Zhong, E. D., Zielinski, M., Žídek, A., Bapst, V., Kohli, P., Jaderberg, M., Hassabis, D. & Jumper, J. M. (2024). Accurate structure prediction of biomolecular interactions with AlphaFold 3. Nature. **630**, 493-500. https://doi.org/10.1038/s41586-024-07487-w.

[6] Tunyasuvunakool, K., Adler, J., Wu, Z., Green, T., Zielinski, M., Zidek, A., Bridgland, A., Cowie, A., Meyer, C., Laydon, A., Velankar, S., Kleywegt, G. J., Bateman, A., Evans, R., Pritzel, A., Figurnov, M., Ronneberger, O., Bates, R., Kohl, S. A. A., Potapenko, A., Ballard, A. J., Romera-Paredes, B., Nikolov, S., Jain, R., Clancy, E., Reiman, D., Petersen, S., Senior, A. W., Kavukcuoglu, K., Birney, E., Kohli, P., Jumper, J. & Hassabis, D. (2021). Highly accurate protein structure prediction for the human proteome. Nature. **596**, 590-596. https://doi.org/10.1038/s41586-021-03828-1.

[7] Jumper, J., Evans, R., Pritzel, A., Green, T., Figurnov, M., Ronneberger, O., Tunyasuvunakool, K., Bates, R., Zidek, A., Potapenko, A., Bridgland, A., Meyer, C., Kohl, S. A. A., Ballard, A. J., Cowie, A., Romera-Paredes, B., Nikolov, S., Jain, R., Adler, J., Back, T., Petersen, S., Reiman, D., Clancy, E., Zielinski, M., Steinegger, M., Pacholska, M., Berghammer, T., Bodenstein, S., Silver, D., Vinyals, O., Senior, A. W., Kavukcuoglu, K., Kohli, P. & Hassabis, D. (2021). Highly accurate protein structure prediction with AlphaFold. Nature. **596**, 583-589. https://doi.org/10.1038/s41586-021-03819-2.

[8] Noda, N. N. & Fujioka, Y. (2015). Atg1 family kinases in autophagy initiation. Cell. Mol. Life Sci. **72**, 3083-3096. https://doi.org/10.1007/s00018-015-1917-z.

[9] Mizushima, N. (2010). The role of the Atg1/ULK1 complex in autophagy regulation. Curr. Opin. Cell Biol. **22**, 132-139. https://doi.org/10.1016/j.ceb.2009.12.004.

[10] Jao, C. C., Ragusa, M. J., Stanley, R. E. & Hurley, J. H. (2013). A HORMA domain in Atg13 mediates PI 3-kinase recruitment in autophagy. Proc Natl Acad Sci U S A. **110**, 5486-5491. https://doi.org/10.1073/pnas.1220306110.

[11] Fujioka, Y., Suzuki, S. W., Yamamoto, H., Kondo-Kakuta, C., Kimura, Y., Hirano, H., Akada, R., Inagaki, F., Ohsumi, Y. & Noda, N. N. (2014). Structural basis of starvation-induced assembly of the autophagy initiation complex. Nat. Struct. Mol. Biol. **21**, 513-521. https://doi.org/10.1038/nsmb.2822.

[12] Kodera, N., Noshiro, D., Dora, S. K., Mori, T., Habchi, J., Blocquel, D., Gruet, A., Dosnon, M., Salladini, E., Bignon, C., Fujioka, Y., Oda, T., Noda, N. N., Sato, M., Lotti, M., Mizuguchi, M., Longhi, S. & Ando, T. (2021). Structural and dynamics analysis of intrinsically disordered proteins by high-speed atomic force microscopy. Nat Nanotechnol. **16**, 181-189. https://doi.org/10.1038/s41565-020-00798-9.

[13] Yamamoto, H., Fujioka, Y., Suzuki, S. W., Noshiro, D., Suzuki, H., Kondo-Kakuta, C., Kimura, Y., Hirano, H., Ando, T., Noda, N. N. & Ohsumi, Y. (2016). The Intrinsically Disordered Protein Atg13 Mediates Supramolecular Assembly of Autophagy Initiation Complexes. Dev. Cell. **38**, 86-99. https://doi.org/10.1016/j.devcel.2016.06.015.

[14] Ragusa, M. J., Stanley, R. E. & Hurley, J. H. (2012). Architecture of the Atg17 complex as a scaffold for autophagosome biogenesis. Cell. **151**, 1501-1512. https://doi.org/10.1016/j.cell.2012.11.028.

[15] Mao, K., Chew, L. H., Inoue-Aono, Y., Cheong, H., Nair, U., Popelka, H., Yip, C. K. & Klionsky, D. J. (2013). Atg29 phosphorylation regulates coordination of the Atg17-Atg31-Atg29 complex with the Atg11 scaffold during autophagy initiation. Proc Natl Acad Sci U S A. **110**, E2875-2884. https://doi.org/10.1073/pnas.1300064110.

[16] Fujioka, Y., Alam, J. M., Noshiro, D., Mouri, K., Ando, T., Okada, Y., May, A. I., Knorr, R. L., Suzuki, K., Ohsumi, Y. & Noda, N. N. (2020). Phase separation organizes the site of autophagosome formation. Nature. **578**, 301-305. https://doi.org/10.1038/s41586-020-1977-6.

[17] Fujioka, Y., Tsuji, T., Kotani, T., Kumeta, H., Kakuta, C., Fujimoto, T., Nakatogawa, H. & Noda, N. N. (2024). Phase separation promotes Atg8 lipidation for autophagy progression. bioRxiv. https://doi.org/https://doi.org/10.1101/2024.08.29.610189.

[18] Kamada, Y., Funakoshi, T., Shintani, T., Nagano, K., Ohsumi, M. & Ohsumi, Y. (2000). Tor-mediated induction of autophagy via an Apg1 protein kinase complex. J. Cell Biol. **150**, 1507-1513. https://doi.org/10.1083/jcb.150.6.1507.

[19] Kim, B. W., Jin, Y., Kim, J., Kim, J. H., Jung, J., Kang, S., Kim, I. Y., Kim, J., Cheong, H. & Song, H.

K. (2018). The C-terminal region of ATG101 bridges ULK1 and PtdIns3K complex in autophagy initiation. Autophagy. **14**, 2104-2116. https://doi.org/10.1080/15548627.2018.1504716.

[20] Suzuki, H., Kaizuka, T., Mizushima, N. & Noda, N. N. (2015). Structure of the Atg101-Atg13 complex reveals essential roles of Atg101 in autophagy initiation. Nat. Struct. Mol. Biol. **22**, 572-580. https://doi.org/10.1038/nsmb.3036.

[21] Michel, M., Schwarten, M., Decker, C., Nagel-Steger, L., Willbold, D. & Weiergraber, O. H. (2015). The mammalian autophagy initiator complex contains 2 HORMA domain proteins. Autophagy. **11**, 2300-2308. https://doi.org/10.1080/15548627.2015.1076605.

[22] Qi, S., Kim, D. J., Stjepanovic, G. & Hurley, J. H. (2015). Structure of the Human Atg13-Atg101 HORMA Heterodimer: an Interaction Hub within the ULK1 Complex. Structure. **23**, 1848-1857. https://doi.org/10.1016/j.str.2015.07.011.

[23] Hosokawa, N., Sasaki, T., Iemura, S., Natsume, T., Hara, T. & Mizushima, N. (2009). Atg101, a novel mammalian autophagy protein interacting with Atg13. Autophagy. **5**, 973-979. https://doi.org/10.4161/auto.5.7.9296.

[24] Mercer, C. A., Kaliappan, A. & Dennis, P. B. (2009). A novel, human Atg13 binding protein, Atg101, interacts with ULK1 and is essential for macroautophagy. Autophagy. **5**, 649-662. https://doi.org/10.4161/auto.5.5.8249.

[25] Ren, X., Nguyen, T. N., Lam, W. K., Buffalo, C. Z., Lazarou, M., Yokom, A. L. & Hurley, J. H. (2023). Structural basis for ATG9A recruitment to the ULK1 complex in mitophagy initiation. Sci Adv. **9**, eadg2997. https://doi.org/10.1126/sciadv.adg2997.

[26] Nguyen, A., Lugarini, F., David, C., Hosnani, P., Alagoz, C., Friedrich, A., Schlutermann, D., Knotkova, B., Patel, A., Parfentev, I., Urlaub, H., Meinecke, M., Stork, B. & Faesen, A. C. (2023). Metamorphic proteins at the basis of human autophagy initiation and lipid transfer. Mol. Cell. **83**, 2077-2090 e2012. https://doi.org/10.1016/j.molcel.2023.04.026.

[27] Chen, M., Nguyen, T. N., Ren, X., Khuu, G., Cook, A. S. I., Zhao, Y., Yildiz, A., Lazarou, M. & Hurley, J. H. (2023). Structure and activation of the human autophagy-initiating ULK1C:PI3KC3-C1 supercomplex. bioRxiv. https://doi.org/https://doi.org/10.1101/2023.06.01.543278.

[28] Hama, Y., Fujioka, Y., Yamamoto, H., Mizushima, N. & Noda, N. N. (2024). The triad interaction of ULK1, ATG13, and FIP200 is required for ULK complex formation and autophagy. eLife. **reviewed preprint**. https://doi.org/https://doi.org/10.7554/eLife.101531.1.

[29] Shi, X., Yokom, A. L., Wang, C., Young, L. N., Youle, R. J. & Hurley, J. H. (2020). ULK complex organization in autophagy by a C-shaped FIP200 N-terminal domain dimer. J. Cell Biol. **219**. https://doi.org/10.1083/jcb.201911047.

[30] Turco, E., Witt, M., Abert, C., Bock-Bierbaum, T., Su, M. Y., Trapannone, R., Sztacho, M., Danieli, A., Shi, X., Zaffagnini, G., Gamper, A., Schuschnig, M., Fracchiolla, D., Bernklau, D., Romanov, J., Hartl, M., Hurley, J. H., Daumke, O. & Martens, S. (2019). FIP200 Claw Domain Binding to p62

Promotes Autophagosome Formation at Ubiquitin Condensates. Mol. Cell. **74**, 330-346 e311. https://doi.org/10.1016/j.molcel.2019.01.035.

[31] Shi, X., Chang, C., Yokom, A. L., Jensen, L. E. & Hurley, J. H. (2020). The autophagy adaptor NDP52 and the FIP200 coiled-coil allosterically activate ULK1 complex membrane recruitment. Elife. **9**. https://doi.org/10.7554/eLife.59099.

[32] Zheng, Q., Chen, Y., Chen, D., Zhao, H., Feng, Y., Meng, Q., Zhao, Y. & Zhang, H. (2022). Calcium transients on the ER surface trigger liquid-liquid phase separation of FIP200 to specify autophagosome initiation sites. Cell. **185**, 4082-4098 e4022. https://doi.org/10.1016/j.cell.2022.09.001.

[33] Kihara, A., Noda, T., Ishihara, N. & Ohsumi, Y. (2001). Two distinct Vps34 phosphatidylinositol 3-kinase complexes function in autophagy and carboxypeptidase Y sorting in Saccharomyces cerevisiae. J. Cell Biol. **152**, 519-530. https://doi.org/10.1083/jcb.152.3.519.

[34] Araki, Y., Ku, W. C., Akioka, M., May, A. I., Hayashi, Y., Arisaka, F., Ishihama, Y. & Ohsumi, Y. (2013). Atg38 is required for autophagy-specific phosphatidylinositol 3-kinase complex integrity. J. Cell Biol. **203**, 299-313. https://doi.org/10.1083/jcb.201304123.

[35] Cao, Y., Wang, Y., Abi Saab, W. F., Yang, F., Pessin, J. E. & Backer, J. M. (2014). NRBF2 regulates macroautophagy as a component of Vps34 Complex I. Biochem. J. **461**, 315-322. https://doi.org/10.1042/BJ20140515.

[36] Lu, J., He, L., Behrends, C., Araki, M., Araki, K., Jun Wang, Q., Catanzaro, J. M., Friedman, S. L., Zong, W. X., Fiel, M. I., Li, M. & Yue, Z. (2014). NRBF2 regulates autophagy and prevents liver injury by modulating Atg14L-linked phosphatidylinositol-3 kinase III activity. Nat Commun. **5**, 3920. https://doi.org/10.1038/ncomms4920.

[37] Baskaran, S., Carlson, L. A., Stjepanovic, G., Young, L. N., Kim, D. J., Grob, P., Stanley, R. E., Nogales, E. & Hurley, J. H. (2014). Architecture and dynamics of the autophagic phosphatidylinositol 3-kinase complex. Elife. **3**. https://doi.org/10.7554/eLife.05115.

[38] Rostislavleva, K., Soler, N., Ohashi, Y., Zhang, L., Pardon, E., Burke, J. E., Masson, G. R., Johnson, C., Steyaert, J., Ktistakis, N. T. & Williams, R. L. (2015). Structure and flexibility of the endosomal Vps34 complex reveals the basis of its function on membranes. Science. **350**, aac7365. https://doi.org/10.1126/science.aac7365.

[39] Ma, M., Liu, J. J., Li, Y., Huang, Y., Ta, N., Chen, Y., Fu, H., Ye, M. D., Ding, Y., Huang, W., Wang, J., Dong, M. Q., Yu, L. & Wang, H. W. (2017). Cryo-EM structure and biochemical analysis reveal the basis of the functional difference between human PI3KC3-C1 and -C2. Cell Res. **27**, 989-1001. https://doi.org/10.1038/cr.2017.94.

[40] Fan, W., Nassiri, A. & Zhong, Q. (2011). Autophagosome targeting and membrane curvature sensing by Barkor/Atg14(L). Proc Natl Acad Sci U S A. **108**, 7769-7774. https://doi.org/10.1073/pnas.1016472108.

[41] Noda, N. N., Kobayashi, T., Adachi, W., Fujioka, Y., Ohsumi, Y. & Inagaki, F. (2012). Structure of the novel C-terminal domain of vacuolar protein sorting 30/autophagy-related protein 6 and its specific role in autophagy. J. Biol. Chem. **287**, 16256-16266. https://doi.org/10.1074/jbc.M112.348250.

[42] Huang, W., Choi, W., Hu, W., Mi, N., Guo, Q., Ma, M., Liu, M., Tian, Y., Lu, P., Wang, F. L., Deng, H., Liu, L., Gao, N., Yu, L. & Shi, Y. (2012). Crystal structure and biochemical analyses reveal Beclin 1 as a novel membrane binding protein. Cell Res. **22**, 473-489. https://doi.org/10.1038/cr.2012.24.

[43] Ohashi, Y., Soler, N., Garcia Ortegon, M., Zhang, L., Kirsten, M. L., Perisic, O., Masson, G. R., Burke, J. E., Jakobi, A. J., Apostolakis, A. A., Johnson, C. M., Ohashi, M., Ktistakis, N. T., Sachse, C. & Williams, R. L. (2016). Characterization of Atg38 and NRBF2, a fifth subunit of the autophagic Vps34/PIK3C3 complex. Autophagy. **12**, 2129-2144. https://doi.org/10.1080/15548627.2016.1226736.

[44] Young, L. N., Cho, K., Lawrence, R., Zoncu, R. & Hurley, J. H. (2016). Dynamics and architecture of the NRBF2-containing phosphatidylinositol 3-kinase complex I of autophagy. Proc Natl Acad Sci U S A. **113**, 8224-8229. https://doi.org/10.1073/pnas.1603650113.

[45] Young, L. N., Goerdeler, F. & Hurley, J. H. (2019). Structural pathway for allosteric activation of the autophagic PI 3-kinase complex I. Proc Natl Acad Sci U S A. **116**, 21508-21513. https://doi.org/10.1073/pnas.1911612116.

[46] Hitomi, K., Kotani, T., Noda, N. N., Kimura, Y. & Nakatogawa, H. (2023). The Atg1 complex, Atg9, and Vac8 recruit PI3K complex I to the pre-autophagosomal structure. J. Cell Biol. **222**. https://doi.org/10.1083/jcb.202210017.

[47] Obara, K., Sekito, T., Niimi, K. & Ohsumi, Y. (2008). The Atg18-Atg2 complex is recruited to autophagic membranes via phosphatidylinositol 3-phosphate and exerts an essential function. J. Biol. Chem. **283**, 23972-23980. https://doi.org/10.1074/jbc.M803180200.

[48] Michell, R. H., Heath, V. L., Lemmon, M. A. & Dove, S. K. (2006). Phosphatidylinositol 3,5-bisphosphate: metabolism and cellular functions. Trends Biochem. Sci. **31**, 52-63. https://doi.org/10.1016/j.tibs.2005.11.013.

[49] Noda, N. N. (2021). Atg2 and Atg9: Intermembrane and interleaflet lipid transporters driving autophagy. Biochim Biophys Acta Mol Cell Biol Lipids. **1866**, 158956. https://doi.org/10.1016/j.bbalip.2021.158956.

[50] Osawa, T., Matoba, K. & Noda, N. N. (2022). Lipid Transport from Endoplasmic Reticulum to Autophagic Membranes. Cold Spring Harb Perspect Biol. **14**. https://doi.org/10.1101/cshperspect.a041254.

[51] Yamamoto, H., Kakuta, S., Watanabe, T. M., Kitamura, A., Sekito, T., Kondo-Kakuta, C., Ichikawa, R., Kinjo, M. & Ohsumi, Y. (2012). Atg9 vesicles are an important membrane source during early steps of autophagosome formation. J. Cell Biol. **198**, 219-233.

https://doi.org/10.1083/jcb.201202061.

[52] Gomez-Sanchez, R., Rose, J., Guimaraes, R., Mari, M., Papinski, D., Rieter, E., Geerts, W. J., Hardenberg, R., Kraft, C., Ungermann, C. & Reggiori, F. (2018). Atg9 establishes Atg2-dependent contact sites between the endoplasmic reticulum and phagophores. J. Cell Biol. **217**, 2743-2763. https://doi.org/10.1083/jcb.201710116.

[53] Mari, M., Griffith, J., Rieter, E., Krishnappa, L., Klionsky, D. J. & Reggiori, F. (2010). An Atg9-containing compartment that functions in the early steps of autophagosome biogenesis. J. Cell Biol. **190**, 1005-1022. https://doi.org/10.1083/jcb.200912089.

[54] Young, A. R., Chan, E. Y., Hu, X. W., Kochl, R., Crawshaw, S. G., High, S., Hailey, D. W., Lippincott-Schwartz, J. & Tooze, S. A. (2006). Starvation and ULK1-dependent cycling of mammalian Atg9 between the TGN and endosomes. J. Cell Sci. **119**, 3888-3900. https://doi.org/10.1242/jcs.03172.

[55] Mattera, R., Park, S. Y., De Pace, R., Guardia, C. M. & Bonifacino, J. S. (2017). AP-4 mediates export of ATG9A from the trans-Golgi network to promote autophagosome formation. Proc Natl Acad Sci U S A. **114**, E10697-E10706. https://doi.org/10.1073/pnas.1717327114.

[56] Orsi, A., Razi, M., Dooley, H. C., Robinson, D., Weston, A. E., Collinson, L. M. & Tooze, S. A. (2012). Dynamic and transient interactions of Atg9 with autophagosomes, but not membrane integration, are required for autophagy. Mol Biol Cell. **23**, 1860-1873. https://doi.org/10.1091/mbc.E11-09-0746.

[57] Broadbent, D. G., Barnaba, C., Perez, G. I. & Schmidt, J. C. (2023). Quantitative analysis of autophagy reveals the role of ATG9 and ATG2 in autophagosome formation. J. Cell Biol. **222**. https://doi.org/10.1083/jcb.202210078.

[58] Olivas, T. J., Wu, Y., Yu, S., Luan, L., Choi, P., Guinn, E. D., Nag, S., De Camilli, P. V., Gupta, K. & Melia, T. J. (2023). ATG9 vesicles comprise the seed membrane of mammalian autophagosomes. J. Cell Biol. **222**. https://doi.org/10.1083/jcb.202208088.

[59] Guardia, C. M., Tan, X. F., Lian, T., Rana, M. S., Zhou, W., Christenson, E. T., Lowry, A. J., Faraldo-Gomez, J. D., Bonifacino, J. S., Jiang, J. & Banerjee, A. (2020). Structure of Human ATG9A, the Only Transmembrane Protein of the Core Autophagy Machinery. Cell Rep. **31**, 107837. https://doi.org/10.1016/j.celrep.2020.107837.

[60] Matoba, K., Kotani, T., Tsutsumi, A., Tsuji, T., Mori, T., Noshiro, D., Sugita, Y., Nomura, N., Iwata, S., Ohsumi, Y., Fujimoto, T., Nakatogawa, H., Kikkawa, M. & Noda, N. N. (2020). Atg9 is a lipid scramblase that mediates autophagosomal membrane expansion. Nat. Struct. Mol. Biol. **27**, 1185-1193. https://doi.org/10.1038/s41594-020-00518-w.

[61] Maeda, S., Yamamoto, H., Kinch, L. N., Garza, C. M., Takahashi, S., Otomo, C., Grishin, N. V., Forli, S., Mizushima, N. & Otomo, T. (2020). Structure, lipid scrambling activity and role in autophagosome formation of ATG9A. Nat. Struct. Mol. Biol. **27**, 1194-1201. https://doi.org/10.1038/s41594-020-00520-2.

[62] Suzuki, S. W., Yamamoto, H., Oikawa, Y., Kondo-Kakuta, C., Kimura, Y., Hirano, H. & Ohsumi, Y.

(2015). Atg13 HORMA domain recruits Atg9 vesicles during autophagosome formation. Proc Natl Acad Sci U S A. **112**, 3350-3355. https://doi.org/10.1073/pnas.1421092112.

[63] Ghanbarpour, A., Valverde, D. P., Melia, T. J. & Reinisch, K. M. (2021). A model for a partnership of lipid transfer proteins and scramblases in membrane expansion and organelle biogenesis. Proc Natl Acad Sci U S A. **118**. https://doi.org/10.1073/pnas.2101562118.

[64] Matoba, K. & Noda, N. N. (2020). Secret of Atg9: lipid scramblase activity drives de novo autophagosome biogenesis. Cell Death Differ. **27**, 3386-3388. https://doi.org/10.1038/s41418-020-00663-1.

[65] Kotani, T., Kirisako, H., Koizumi, M., Ohsumi, Y. & Nakatogawa, H. (2018). The Atg2-Atg18 complex tethers pre-autophagosomal membranes to the endoplasmic reticulum for autophagosome formation. Proc Natl Acad Sci U S A. **115**, 10363-10368. https://doi.org/10.1073/pnas.1806727115.

[66] Suzuki, K., Akioka, M., Kondo-Kakuta, C., Yamamoto, H. & Ohsumi, Y. (2013). Fine mapping of autophagy-related proteins during autophagosome formation in Saccharomyces cerevisiae. J. Cell Sci. **126**, 2534-2544. https://doi.org/10.1242/jcs.122960.

[67] Graef, M., Friedman, J. R., Graham, C., Babu, M. & Nunnari, J. (2013). ER exit sites are physical and functional core autophagosome biogenesis components. Mol Biol Cell. **24**, 2918-2931. https://doi.org/10.1091/mbc.E13-07-0381.

[68] Osawa, T., Ishii, Y. & Noda, N. N. (2020). Human ATG2B possesses a lipid transfer activity which is accelerated by negatively charged lipids and WIPI4. Genes Cells. **25**, 65-70. https://doi.org/10.1111/gtc.12733.

[69] Osawa, T., Kotani, T., Kawaoka, T., Hirata, E., Suzuki, K., Nakatogawa, H., Ohsumi, Y. & Noda, N. N. (2019). Atg2 mediates direct lipid transfer between membranes for autophagosome formation. Nat. Struct. Mol. Biol. **26**, 281-288. https://doi.org/10.1038/s41594-019-0203-4.

[70] Maeda, S., Otomo, C. & Otomo, T. (2019). The autophagic membrane tether ATG2A transfers lipids between membranes. Elife. **8**. https://doi.org/10.7554/eLife.45777.

[71] Valverde, D. P., Yu, S., Boggavarapu, V., Kumar, N., Lees, J. A., Walz, T., Reinisch, K. M. & Melia, T. J. (2019). ATG2 transports lipids to promote autophagosome biogenesis. J. Cell Biol. **218**, 1787-1798. https://doi.org/10.1083/jcb.201811139.

[72] Wang, Y., Dahmane, S., Ti, R., Mai, X., Zhu, L., Carlson, L. A. & Stjepanovic, G. (2024). Structural basis for lipid transfer by the ATG2A-ATG9A complex. Nat. Struct. Mol. Biol. https://doi.org/10.1038/s41594-024-01376-6.

[73] van Vliet, A. R., Chiduza, G. N., Maslen, S. L., Pye, V. E., Joshi, D., De Tito, S., Jefferies, H. B. J., Christodoulou, E., Roustan, C., Punch, E., Hervas, J. H., O'Reilly, N., Skehel, J. M., Cherepanov, P. & Tooze, S. A. (2022). ATG9A and ATG2A form a heteromeric complex essential for autophagosome formation. Mol. Cell. **82**, 4324-4339 e4328. https://doi.org/10.1016/j.molcel.2022.10.017.

[74] Chowdhury, S., Otomo, C., Leitner, A., Ohashi, K., Aebersold, R., Lander, G. C. & Otomo, T. (2018). Insights into autophagosome biogenesis from structural and biochemical analyses of the ATG2A-WIPI4 complex. Proc Natl Acad Sci U S A. **115**, E9792-E9801. https://doi.org/10.1073/pnas.1811874115.

[75] Zheng, J. X., Li, Y., Ding, Y. H., Liu, J. J., Zhang, M. J., Dong, M. Q., Wang, H. W. & Yu, L. (2017). Architecture of the ATG2B-WDR45 complex and an aromatic Y/HF motif crucial for complex formation. Autophagy. **13**, 1870-1883. https://doi.org/10.1080/15548627.2017.1359381.

[76] Lees, J. A. & Reinisch, K. M. (2020). Inter-organelle lipid transfer: a channel model for Vps13 and chorein-N motif proteins. Curr. Opin. Cell Biol. **65**, 66-71. https://doi.org/10.1016/j.ceb.2020.02.008.

[77] Osawa, T. & Noda, N. N. (2019). Atg2: A novel phospholipid transfer protein that mediates de novo autophagosome biogenesis. Protein Sci. **28**, 1005-1012. https://doi.org/10.1002/pro.3623.

[78] Schutter, M., Giavalisco, P., Brodesser, S. & Graef, M. (2020). Local Fatty Acid Channeling into Phospholipid Synthesis Drives Phagophore Expansion during Autophagy. Cell. **180**, 135-149 e114. https://doi.org/10.1016/j.cell.2019.12.005.

[79] Orii, M., Tsuji, T., Ogasawara, Y. & Fujimoto, T. (2021). Transmembrane phospholipid translocation mediated by Atg9 is involved in autophagosome formation. J. Cell Biol. **220**. https://doi.org/10.1083/jcb.202009194.

[80] Ichimura, Y., Kirisako, T., Takao, T., Satomi, Y., Shimonishi, Y., Ishihara, N., Mizushima, N., Tanida, I., Kominami, E., Ohsumi, M., Noda, T. & Ohsumi, Y. (2000). A ubiquitin-like system mediates protein lipidation. Nature. **408**, 488-492. https://doi.org/10.1038/35044114.

[81] Mizushima, N., Noda, T., Yoshimori, T., Tanaka, Y., Ishii, T., George, M. D., Klionsky, D. J., Ohsumi, M. & Ohsumi, Y. (1998). A protein conjugation system essential for autophagy. Nature. **395**, 395-398. https://doi.org/10.1038/26506.

[82] Xie, Z., Nair, U. & Klionsky, D. J. (2008). Atg8 controls phagophore expansion during autophagosome formation. Mol Biol Cell. **19**, 3290-3298. https://doi.org/10.1091/mbc.E07-12-1292.

[83] Nakatogawa, H., Ichimura, Y. & Ohsumi, Y. (2007). Atg8, a ubiquitin-like protein required for autophagosome formation, mediates membrane tethering and hemifusion. Cell. **130**, 165-178. https://doi.org/10.1016/j.cell.2007.05.021.

[84] Suzuki, N. N., Yoshimoto, K., Fujioka, Y., Ohsumi, Y. & Inagaki, F. (2005). The crystal structure of plant ATG12 and its biological implication in autophagy. Autophagy. **1**, 119-126. https://doi.org/10.4161/auto.1.2.1859.

[85] Noda, N. N., Satoo, K., Fujioka, Y., Kumeta, H., Ogura, K., Nakatogawa, H., Ohsumi, Y. & Inagaki, F. (2011). Structural basis of Atg8 activation by a homodimeric E1, Atg7. Mol. Cell. **44**, 462-475. https://doi.org/10.1016/j.molcel.2011.08.035.

[86] Taherbhoy, A. M., Tait, S. W., Kaiser, S. E., Williams, A. H., Deng, A., Nourse, A., Hammel, M.,

Kurinov, I., Rock, C. O., Green, D. R. & Schulman, B. A. (2011). Atg8 transfer from Atg7 to Atg3: a distinctive E1-E2 architecture and mechanism in the autophagy pathway. Mol. Cell. **44**, 451-461. https://doi.org/10.1016/j.molcel.2011.08.034.

[87] Hong, S. B., Kim, B. W., Lee, K. E., Kim, S. W., Jeon, H., Kim, J. & Song, H. K. (2011). Insights into noncanonical E1 enzyme activation from the structure of autophagic E1 Atg7 with Atg8. Nat. Struct. Mol. Biol. **18**, 1323-1330. https://doi.org/10.1038/nsmb.2165.

[88] Yamaguchi, M., Matoba, K., Sawada, R., Fujioka, Y., Nakatogawa, H., Yamamoto, H., Kobashigawa, Y., Hoshida, H., Akada, R., Ohsumi, Y., Noda, N. N. & Inagaki, F. (2012). Noncanonical recognition and UBL loading of distinct E2s by autophagy-essential Atg7. Nat. Struct. Mol. Biol. **19**, 1250-1256. https://doi.org/10.1038/nsmb.2451.

[89] Kaiser, S. E., Mao, K., Taherbhoy, A. M., Yu, S., Olszewski, J. L., Duda, D. M., Kurinov, I., Deng, A., Fenn, T. D., Klionsky, D. J. & Schulman, B. A. (2012). Noncanonical E2 recruitment by the autophagy E1 revealed by Atg7-Atg3 and Atg7-Atg10 structures. Nat. Struct. Mol. Biol. **19**, 1242-1249. https://doi.org/10.1038/nsmb.2415.

[90] Yamaguchi, M., Noda, N. N., Yamamoto, H., Shima, T., Kumeta, H., Kobashigawa, Y., Akada, R., Ohsumi, Y. & Inagaki, F. (2012). Structural insights into Atg10-mediated formation of the autophagy-essential Atg12-Atg5 conjugate. Structure. **20**, 1244-1254. https://doi.org/10.1016/j.str.2012.04.018.

[91] Hong, S. B., Kim, B. W., Kim, J. H. & Song, H. K. (2012). Structure of the autophagic E2 enzyme Atg10. Acta Crystallogr D Biol Crystallogr. **68**, 1409-1417. https://doi.org/10.1107/S0907444912034166.

[92] Noda, N. N., Fujioka, Y., Hanada, T., Ohsumi, Y. & Inagaki, F. (2013). Structure of the Atg12-Atg5 conjugate reveals a platform for stimulating Atg8-PE conjugation. EMBO Rep. **14**, 206-211. https://doi.org/10.1038/embor.2012.208.

[93] Otomo, C., Metlagel, Z., Takaesu, G. & Otomo, T. (2013). Structure of the human ATG12~ATG5 conjugate required for LC3 lipidation in autophagy. Nat. Struct. Mol. Biol. **20**, 59-66. https://doi.org/10.1038/nsmb.2431.

[94] Matsushita, M., Suzuki, N. N., Obara, K., Fujioka, Y., Ohsumi, Y. & Inagaki, F. (2007). Structure of Atg5.Atg16, a complex essential for autophagy. J. Biol. Chem. **282**, 6763-6772. https://doi.org/10.1074/jbc.M609876200.

[95] Fujioka, Y., Noda, N. N., Nakatogawa, H., Ohsumi, Y. & Inagaki, F. (2010). Dimeric coiled-coil structure of Saccharomyces cerevisiae Atg16 and its functional significance in autophagy. J. Biol. Chem. **285**, 1508-1515. https://doi.org/10.1074/jbc.M109.053520.

[96] Mizushima, N., Noda, T. & Ohsumi, Y. (1999). Apg16p is required for the function of the Apg12p-Apg5p conjugate in the yeast autophagy pathway. EMBO J. **18**, 3888-3896. https://doi.org/10.1093/emboj/18.14.3888.

[97] Harada, K., Kotani, T., Kirisako, H., Sakoh-Nakatogawa, M., Oikawa, Y., Kimura, Y., Hirano, H., Yamamoto, H., Ohsumi, Y. & Nakatogawa, H. (2019). Two distinct mechanisms target the autophagy-related E3 complex to the pre-autophagosomal structure. Elife. **8**. https://doi.org/10.7554/eLife.43088.

[98] Munzel, L., Neumann, P., Otto, F. B., Krick, R., Metje-Sprink, J., Kroppen, B., Karedla, N., Enderlein, J., Meinecke, M., Ficner, R. & Thumm, M. (2021). Atg21 organizes Atg8 lipidation at the contact of the vacuole with the phagophore. Autophagy. **17**, 1458-1478. https://doi.org/10.1080/15548627.2020.1766332.

[99] Juris, L., Montino, M., Rube, P., Schlotterhose, P., Thumm, M. & Krick, R. (2015). PI3P binding by Atg21 organises Atg8 lipidation. EMBO J. **34**, 955-973. https://doi.org/10.15252/embj.201488957.

[100] Mizushima, N., Kuma, A., Kobayashi, Y., Yamamoto, A., Matsubae, M., Takao, T., Natsume, T., Ohsumi, Y. & Yoshimori, T. (2003). Mouse Apg16L, a novel WD-repeat protein, targets to the autophagic isolation membrane with the Apg12-Apg5 conjugate. J. Cell Sci. **116**, 1679-1688. https://doi.org/10.1242/jcs.00381.

[101] Fletcher, K., Ulferts, R., Jacquin, E., Veith, T., Gammoh, N., Arasteh, J. M., Mayer, U., Carding, S. R., Wileman, T., Beale, R. & Florey, O. (2018). The WD40 domain of ATG16L1 is required for its non-canonical role in lipidation of LC3 at single membranes. EMBO J. **37**. https://doi.org/10.15252/embj.201797840.

[102] Lystad, A. H., Carlsson, S. R., de la Ballina, L. R., Kauffman, K. J., Nag, S., Yoshimori, T., Melia, T. J. & Simonsen, A. (2019). Distinct functions of ATG16L1 isoforms in membrane binding and LC3B lipidation in autophagy-related processes. Nat. Cell Biol. **21**, 372-383. https://doi.org/10.1038/s41556-019-0274-9.

[103] Jensen, L. E., Rao, S., Schuschnig, M., Cada, A. K., Martens, S., Hummer, G. & Hurley, J. H. (2022). Membrane curvature sensing and stabilization by the autophagic LC3 lipidation machinery. Sci Adv. **8**, eadd1436. https://doi.org/10.1126/sciadv.add1436.

[104] Dudley, L. J., Cabodevilla, A. G., Makar, A. N., Sztacho, M., Michelberger, T., Marsh, J. A., Houston, D. R., Martens, S., Jiang, X. & Gammoh, N. (2019). Intrinsic lipid binding activity of ATG16L1 supports efficient membrane anchoring and autophagy. EMBO J. **38**. https://doi.org/10.15252/embj.2018100554.

[105] Nishimura, T., Kaizuka, T., Cadwell, K., Sahani, M. H., Saitoh, T., Akira, S., Virgin, H. W. & Mizushima, N. (2013). FIP200 regulates targeting of Atg16L1 to the isolation membrane. EMBO Rep. **14**, 284-291. https://doi.org/10.1038/embor.2013.6.

[106] Strong, L. M., Chang, C., Riley, J. F., Boecker, C. A., Flower, T. G., Buffalo, C. Z., Ren, X., Stavoe, A. K., Holzbaur, E. L. & Hurley, J. H. (2021). Structural basis for membrane recruitment of ATG16L1 by WIPI2 in autophagy. Elife. **10**. https://doi.org/10.7554/eLife.70372.

[107] Fracchiolla, D., Chang, C., Hurley, J. H. & Martens, S. (2020). A PI3K-WIPI2 positive feedback loop

allosterically activates LC3 lipidation in autophagy. J. Cell Biol. **219**. https://doi.org/10.1083/jcb.201912098.

[108] Gong, X., Wang, Y., Tang, Y., Zhang, M., Li, M., Zhang, Y. & Pan, L. (2023). ATG16L1 adopts a dual-binding site mode to interact with WIPI2b in autophagy. Sci Adv. **9**, eadf0824. https://doi.org/10.1126/sciadv.adf0824.

[109] Dooley, H. C., Razi, M., Polson, H. E., Girardin, S. E., Wilson, M. I. & Tooze, S. A. (2014). WIPI2 links LC3 conjugation with PI3P, autophagosome formation, and pathogen clearance by recruiting Atg12-5-16L1. Mol. Cell. **55**, 238-252. https://doi.org/10.1016/j.molcel.2014.05.021.

[110] Hanada, T., Noda, N. N., Satomi, Y., Ichimura, Y., Fujioka, Y., Takao, T., Inagaki, F. & Ohsumi, Y. (2007). The Atg12-Atg5 conjugate has a novel E3-like activity for protein lipidation in autophagy. J. Biol. Chem. **282**, 37298-37302. https://doi.org/10.1074/jbc.C700195200.

[111] Fujioka, Y., Noda, N. N., Fujii, K., Yoshimoto, K., Ohsumi, Y. & Inagaki, F. (2008). In vitro reconstitution of plant Atg8 and Atg12 conjugation systems essential for autophagy. J. Biol. Chem. **283**, 1921-1928. https://doi.org/10.1074/jbc.M706214200.

[112] Rogov, V. V., Nezis, I. P., Tsapras, P., Zhang, H., Dagdas, Y., Noda, N. N., Nakatogawa, H., Wirth, M., Mouilleron, S., McEwan, D. G., Behrends, C., Deretic, V., Elazar, Z., Tooze, S. A., Dikic, I., Lamark, T. & Johansen, T. (2023). Atg8 family proteins, LIR/AIM motifs and other interaction modes. Autophagy Reports. **2**.

[113] Sugawara, K., Suzuki, N. N., Fujioka, Y., Mizushima, N., Ohsumi, Y. & Inagaki, F. (2004). The crystal structure of microtubule-associated protein light chain 3, a mammalian homologue of Saccharomyces cerevisiae Atg8. Genes Cells. **9**, 611-618. https://doi.org/10.1111/j.1356-9597.2004.00750.x.

[114] Bavro, V. N., Sola, M., Bracher, A., Kneussel, M., Betz, H. & Weissenhorn, W. (2002). Crystal structure of the GABA(A)-receptor-associated protein, GABARAP. EMBO Rep. **3**, 183-189. https://doi.org/10.1093/embo-reports/kvf026.

[115] Paz, Y., Elazar, Z. & Fass, D. (2000). Structure of GATE-16, membrane transport modulator and mammalian ortholog of autophagocytosis factor Aut7p. J. Biol. Chem. **275**, 25445-25450. https://doi.org/10.1074/jbc.C000307200.

[116] Kumeta, H., Watanabe, M., Nakatogawa, H., Yamaguchi, M., Ogura, K., Adachi, W., Fujioka, Y., Noda, N. N., Ohsumi, Y. & Inagaki, F. (2010). The NMR structure of the autophagy-related protein Atg8. J. Biomol. NMR. **47**, 237-241. https://doi.org/10.1007/s10858-010-9420-1.

[117] Noda, N. N., Kumeta, H., Nakatogawa, H., Satoo, K., Adachi, W., Ishii, J., Fujioka, Y., Ohsumi, Y. & Inagaki, F. (2008). Structural basis of target recognition by Atg8/LC3 during selective autophagy. Genes Cells. **13**, 1211-1218. https://doi.org/10.1111/j.1365-2443.2008.01238.x.

[118] Rogov, V. V., Stolz, A., Ravichandran, A. C., Rios-Szwed, D. O., Suzuki, H., Kniss, A., Löhr, F., Wakatsuki, S., Dötsch, V., Dikic, I., Dobson, R. C. & McEwan, D. G. (2017). Structural and

functional analysis of the GABARAP interaction motif (GIM). EMBO Rep. **18**, 1382-1396. https://doi.org/10.15252/embr.201643587.

[119] Chino, H., Yamasaki, A., Ode, K. L., Ueda, H. R., Noda, N. N. & Mizushima, N. (2022). Phosphorylation by casein kinase 2 enhances the interaction between ER-phagy receptor TEX264 and ATG8 proteins. EMBO Rep. **23**, e54801. https://doi.org/10.15252/embr.202254801.

[120] Noda, N. N., Ohsumi, Y. & Inagaki, F. (2010). Atg8-family interacting motif crucial for selective autophagy. FEBS Lett. **584**, 1379-1385. https://doi.org/10.1016/j.febslet.2010.01.018.

[121] Birgisdottir, A. B., Lamark, T. & Johansen, T. (2013). The LIR motif - crucial for selective autophagy. J. Cell Sci. **126**, 3237-3247. https://doi.org/10.1242/jcs.126128.

[122] Kirisako, T., Ichimura, Y., Okada, H., Kabeya, Y., Mizushima, N., Yoshimori, T., Ohsumi, M., Takao, T., Noda, T. & Ohsumi, Y. (2000). The reversible modification regulates the membrane-binding state of Apg8/Aut7 essential for autophagy and the cytoplasm to vacuole targeting pathway. J. Cell Biol. **151**, 263-276. https://doi.org/10.1083/jcb.151.2.263.

[123] Abreu, S., Kriegenburg, F., Gomez-Sanchez, R., Mari, M., Sanchez-Wandelmer, J., Skytte Rasmussen, M., Soares Guimaraes, R., Zens, B., Schuschnig, M., Hardenberg, R., Peter, M., Johansen, T., Kraft, C., Martens, S. & Reggiori, F. (2017). Conserved Atg8 recognition sites mediate Atg4 association with autophagosomal membranes and Atg8 deconjugation. EMBO Rep. **18**, 765-780. https://doi.org/10.15252/embr.201643146.

[124] Kumanomidou, T., Mizushima, T., Komatsu, M., Suzuki, A., Tanida, I., Sou, Y. S., Ueno, T., Kominami, E., Tanaka, K. & Yamane, T. (2006). The crystal structure of human Atg4b, a processing and de-conjugating enzyme for autophagosome-forming modifiers. J. Mol. Biol. **355**, 612-618. https://doi.org/10.1016/j.jmb.2005.11.018.

[125] Sugawara, K., Suzuki, N. N., Fujioka, Y., Mizushima, N., Ohsumi, Y. & Inagaki, F. (2005). Structural basis for the specificity and catalysis of human Atg4B responsible for mammalian autophagy. J. Biol. Chem. **280**, 40058-40065. https://doi.org/10.1074/jbc.M509158200.

[126] Satoo, K., Noda, N. N., Kumeta, H., Fujioka, Y., Mizushima, N., Ohsumi, Y. & Inagaki, F. (2009). The structure of Atg4B-LC3 complex reveals the mechanism of LC3 processing and delipidation during autophagy. EMBO J. **28**, 1341-1350. https://doi.org/10.1038/emboj.2009.80.

[127] Agrotis, A., Pengo, N., Burden, J. J. & Ketteler, R. (2019). Redundancy of human ATG4 protease isoforms in autophagy and LC3/GABARAP processing revealed in cells. Autophagy. **15**, 976-997. https://doi.org/10.1080/15548627.2019.1569925.

[128] Yamada, Y., Suzuki, N. N., Hanada, T., Ichimura, Y., Kumeta, H., Fujioka, Y., Ohsumi, Y. & Inagaki, F. (2007). The crystal structure of Atg3, an autophagy-related ubiquitin carrier protein (E2) enzyme that mediates Atg8 lipidation. J. Biol. Chem. **282**, 8036-8043. https://doi.org/10.1074/jbc.M611473200.

[129] Sakoh-Nakatogawa, M., Matoba, K., Asai, E., Kirisako, H., Ishii, J., Noda, N. N., Inagaki, F.,

Nakatogawa, H. & Ohsumi, Y. (2013). Atg12-Atg5 conjugate enhances E2 activity of Atg3 by rearranging its catalytic site. Nat. Struct. Mol. Biol. **20**, 433-439. https://doi.org/10.1038/nsmb.2527.

[130] Zheng, Y., Qiu, Y., Grace, C. R. R., Liu, X., Klionsky, D. J. & Schulman, B. A. (2019). A switch element in the autophagy E2 Atg3 mediates allosteric regulation across the lipidation cascade. Nat Commun. **10**, 3600. https://doi.org/10.1038/s41467-019-11435-y.

[131] Metlagel, Z., Otomo, C., Takaesu, G. & Otomo, T. (2013). Structural basis of ATG3 recognition by the autophagic ubiquitin-like protein ATG12. Proc Natl Acad Sci U S A. **110**, 18844-18849. https://doi.org/10.1073/pnas.1314755110.

[132] Matoba, K. & Noda, N. N. (2021). Atg12-Interacting Motif Is Crucial for E2-E3 Interaction in Plant Atg8 System. Biol. Pharm. Bull. **44**, 1337-1343. https://doi.org/10.1248/bpb.b21-00439.

[133] Nath, S., Dancourt, J., Shteyn, V., Puente, G., Fong, W. M., Nag, S., Bewersdorf, J., Yamamoto, A., Antonny, B. & Melia, T. J. (2014). Lipidation of the LC3/GABARAP family of autophagy proteins relies on a membrane-curvature-sensing domain in Atg3. Nat. Cell Biol. **16**, 415-424. https://doi.org/10.1038/ncb2940.

[134] Hanada, T., Satomi, Y., Takao, T. & Ohsumi, Y. (2009). The amino-terminal region of Atg3 is essential for association with phosphatidylethanolamine in Atg8 lipidation. FEBS Lett. **583**, 1078-1083. https://doi.org/10.1016/j.febslet.2009.03.009.

[135] Nishimura, T., Lazzeri, G., Mizushima, N., Covino, R. & Tooze, S. A. (2023). Unique amphipathic α helix drives membrane insertion and enzymatic activity of ATG3. Sci Adv. **9**, eadh1281. https://doi.org/10.1126/sciadv.adh1281.

[136] Maruyama, T., Alam, J. M., Fukuda, T., Kageyama, S., Kirisako, H., Ishii, Y., Shimada, I., Ohsumi, Y., Komatsu, M., Kanki, T., Nakatogawa, H. & Noda, N. N. (2021). Membrane perturbation by lipidated Atg8 underlies autophagosome biogenesis. Nat. Struct. Mol. Biol. **28**, 583-593. https://doi.org/10.1038/s41594-021-00614-5.

[137] Zhang, W., Nishimura, T., Gahlot, D., Saito, C., Davis, C., Jefferies, H. B. J., Schreiber, A., Thukral, L. & Tooze, S. A. (2023). Autophagosome membrane expansion is mediated by the N-terminus and. Elife. **12**. https://doi.org/10.7554/eLife.89185.

[138] Iriondo, M. N., Etxaniz, A., Varela, Y. R., Ballesteros, U., Lázaro, M., Valle, M., Fracchiolla, D., Martens, S., Montes, L. R., Goñi, F. M. & Alonso, A. (2023). Effect of ATG12-ATG5-ATG16L1 autophagy E3-like complex on the ability of LC3/GABARAP proteins to induce vesicle tethering and fusion. Cell. Mol. Life Sci. **80**, 56. https://doi.org/10.1007/s00018-023-04704-z.

[139] Wu, F., Watanabe, Y., Guo, X. Y., Qi, X., Wang, P., Zhao, H. Y., Wang, Z., Fujioka, Y., Zhang, H., Ren, J. Q., Fang, T. C., Shen, Y. X., Feng, W., Hu, J. J. & Noda, N. N. (2015). Structural Basis of the Differential Function of the Two C. elegans Atg8 Homologs, LGG-1 and LGG-2, in Autophagy. Mol. Cell. **60**, 914-929. https://doi.org/10.1016/j.molcel.2015.11.019.

[140] Weidberg, H., Shpilka, T., Shvets, E., Abada, A., Shimron, F. & Elazar, Z. (2011). LC3 and GATE-16

N termini mediate membrane fusion processes required for autophagosome biogenesis. Dev. Cell. **20**, 444-454. https://doi.org/10.1016/j.devcel.2011.02.006.

[141] Nakatogawa, H., Ishii, J., Asai, E. & Ohsumi, Y. (2012). Atg4 recycles inappropriately lipidated Atg8 to promote autophagosome biogenesis. Autophagy. **8**, 177-186. https://doi.org/10.4161/auto.8.2.18373.

[142] Nair, U., Yen, W. L., Mari, M., Cao, Y., Xie, Z., Baba, M., Reggiori, F. & Klionsky, D. J. (2012). A role for Atg8-PE deconjugation in autophagosome biogenesis. Autophagy. **8**, 780-793. https://doi.org/10.4161/auto.19385.

[143] Yu, Z. Q., Ni, T., Hong, B., Wang, H. Y., Jiang, F. J., Zou, S., Chen, Y., Zheng, X. L., Klionsky, D. J., Liang, Y. & Xie, Z. (2012). Dual roles of Atg8-PE deconjugation by Atg4 in autophagy. Autophagy. **8**, 883-892. https://doi.org/10.4161/auto.19652.

[144] Schreiber, A., Collins, B. C., Davis, C., Enchev, R. I., Sedra, A., D'Antuono, R., Aebersold, R. & Peter, M. (2021). Multilayered regulation of autophagy by the Atg1 kinase orchestrates spatial and temporal control of autophagosome formation. Mol. Cell. **81**, 5066-5081.e5010. https://doi.org/10.1016/j.molcel.2021.10.024.

[145] Hirata, E., Ohya, Y. & Suzuki, K. (2017). Atg4 plays an important role in efficient expansion of autophagic isolation membranes by cleaving lipidated Atg8 in Saccharomyces cerevisiae. PLoS One. **12**, e0181047. https://doi.org/10.1371/journal.pone.0181047.

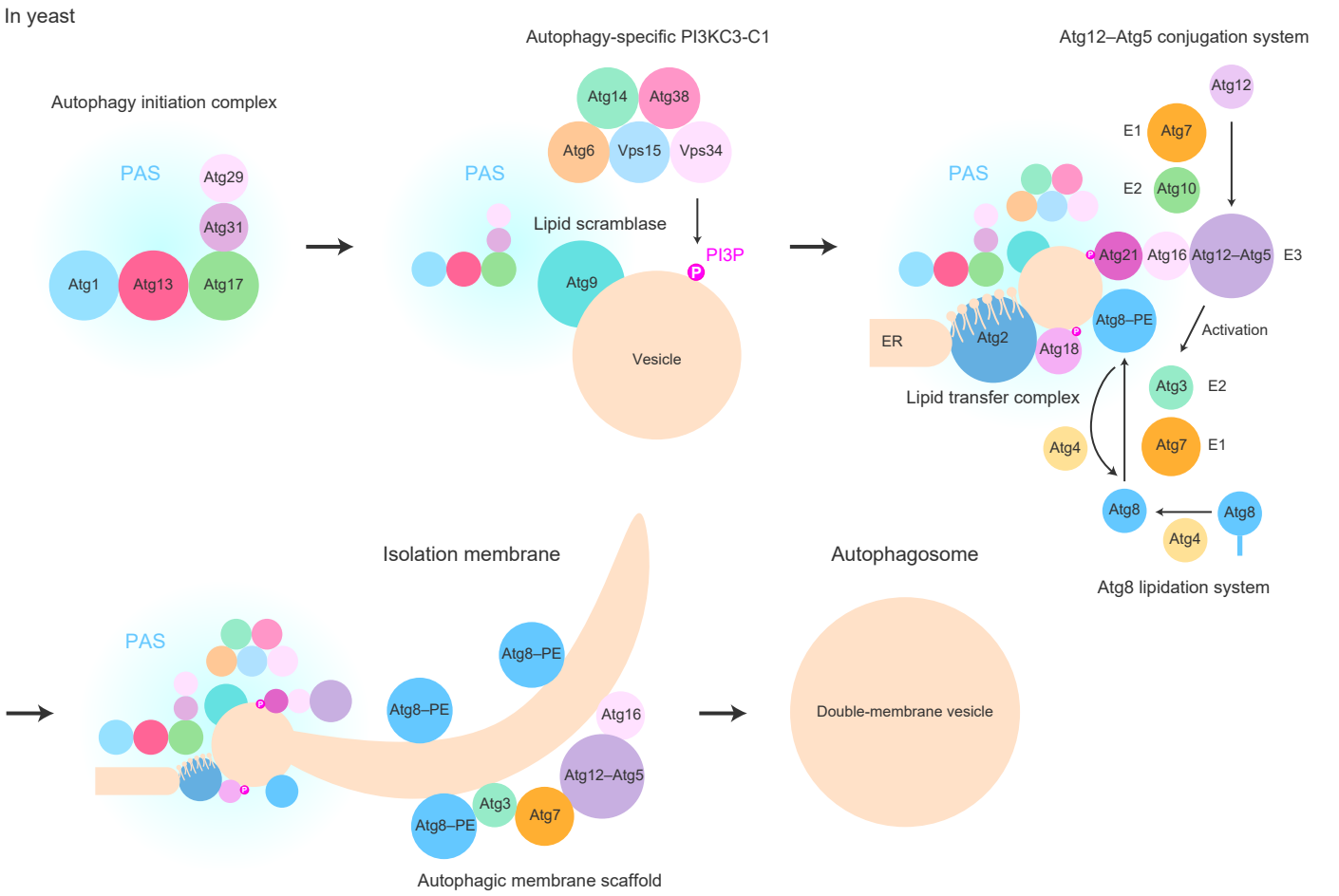
[146] Alam, J. M., Maruyama, T., Noshiro, D., Kakuta, C., Kotani, T., Nakatogawa, H. & Noda, N. N. (2024). Complete set of the Atg8-E1-E2-E3 conjugation machinery forms an interaction web that mediates membrane shaping. Nat. Struct. Mol. Biol. **31**, 170-178. https://doi.org/10.1038/s41594-023-01132-2.

[147] Kaufmann, A., Beier, V., Franquelim, H. G. & Wollert, T. (2014). Molecular mechanism of autophagic membrane-scaffold assembly and disassembly. Cell. **156**, 469-481. https://doi.org/10.1016/j.cell.2013.12.022.

[148] Mohan, J., Moparthi, S. B., Girard-Blanc, C., Campisi, D., Blanchard, S., Nugues, C., Rama, S., Salles, A., Pénard, E., Vassilopoulos, S. & Wollert, T. (2024). ATG16L1 induces the formation of phagophore-like membrane cups. Nat. Struct. Mol. Biol. **31**, 1448-1459. https://doi.org/10.1038/s41594-024-01300-y.

[149] Meng, E. C., Goddard, T. D., Pettersen, E. F., Couch, G. S., Pearson, Z. J., Morris, J. H. & Ferrin, T. E. (2023). UCSF ChimeraX: Tools for structure building and analysis. Protein Sci. **32**, e4792. https://doi.org/10.1002/pro.4792.

Figure 1


In yeast
Autophagy initiation complex
PAS
Atg29
Atg31
Atg1
Atg13
Atg17
Autophagy-specific PI3KC3-C1
Atg14
Atg38
Atg6
Vps15
Vps34
Lipid scramblase
PI3P
Atg9
Vesicle
Atg12–Atg5 conjugation system
Atg12
E1
Atg7
E2
Atg10
Atg21
Atg16
Atg12–Atg5
E3
Atg8–PE
Activation
ER
Atg2
Atg18
Lipid transfer complex
Atg3
E2
Atg4
Atg7
E1
Atg8
Atg8
Atg4
Atg8 lipidation system
Isolation membrane
Autophagosome
Double-membrane vesicle
Atg8–PE
Atg16
Atg12–Atg5
Atg3
Atg7
Autophagic membrane scaffold

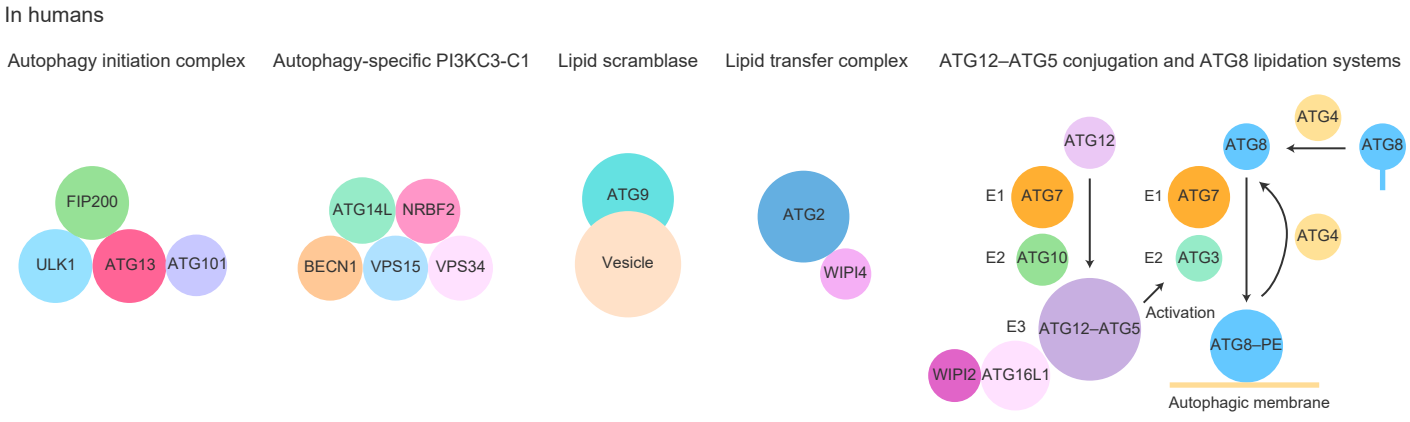

In humans
Autophagy initiation complex
Autophagy-specific PI3KC3-C1
Lipid scramblase
Lipid transfer complex
ATG12–ATG5 conjugation and ATG8 lipidation systems
FIP200
ULK1
ATG13
ATG101
ATG14L
NRBF2
BECN1
VPS15
VPS34
ATG9
Vesicle
ATG2
WIPI4
ATG12
E1
ATG7
E2
ATG10
E3
ATG12–ATG5
WIPI2
ATG16L1
ATG4
ATG8
ATG8
E1
ATG7
E2
ATG3
ATG4
Activation
ATG8–PE
Autophagic membrane

Figure 2

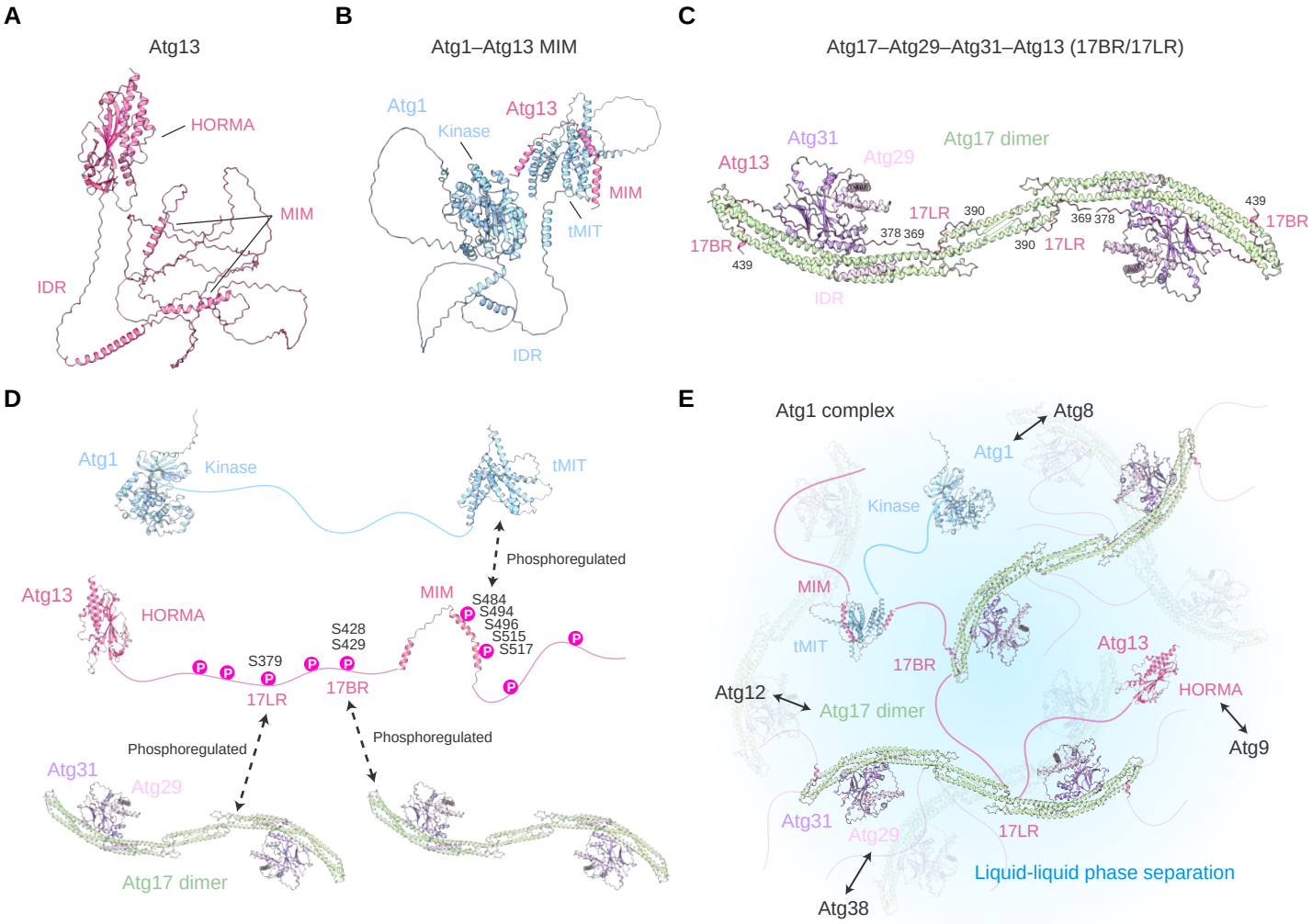

A
Atg13
HORMA
MIM
IDR
B
Atg1–Atg13 MIM
Atg1
Kinase
Atg13
MIM
tMIT
IDR
C
Atg17–Atg29–Atg31–Atg13 (17BR/17LR)
Atg31
Atg17 dimer
Atg13
Atg29
17LR
390
378 369
369 378
439
17BR
17BR
439
390 17LR
IDR
D
Atg1
Kinase
tMIT
Phosphoregulated
Atg13
HORMA
MIM
S484
S494
S496
S515
S517
S428
S429
S379
17LR
17BR
Phosphoregulated
Phosphoregulated
Atg31
Atg29
Atg17 dimer
E
Atg1 complex
Atg8
Atg1
Kinase
MIM
tMIT
17BR
Atg13
Atg12
Atg17 dimer
HORMA
Atg9
Atg31
Atg29
17LR
Liquid-liquid phase separation
Atg38

Figure 3

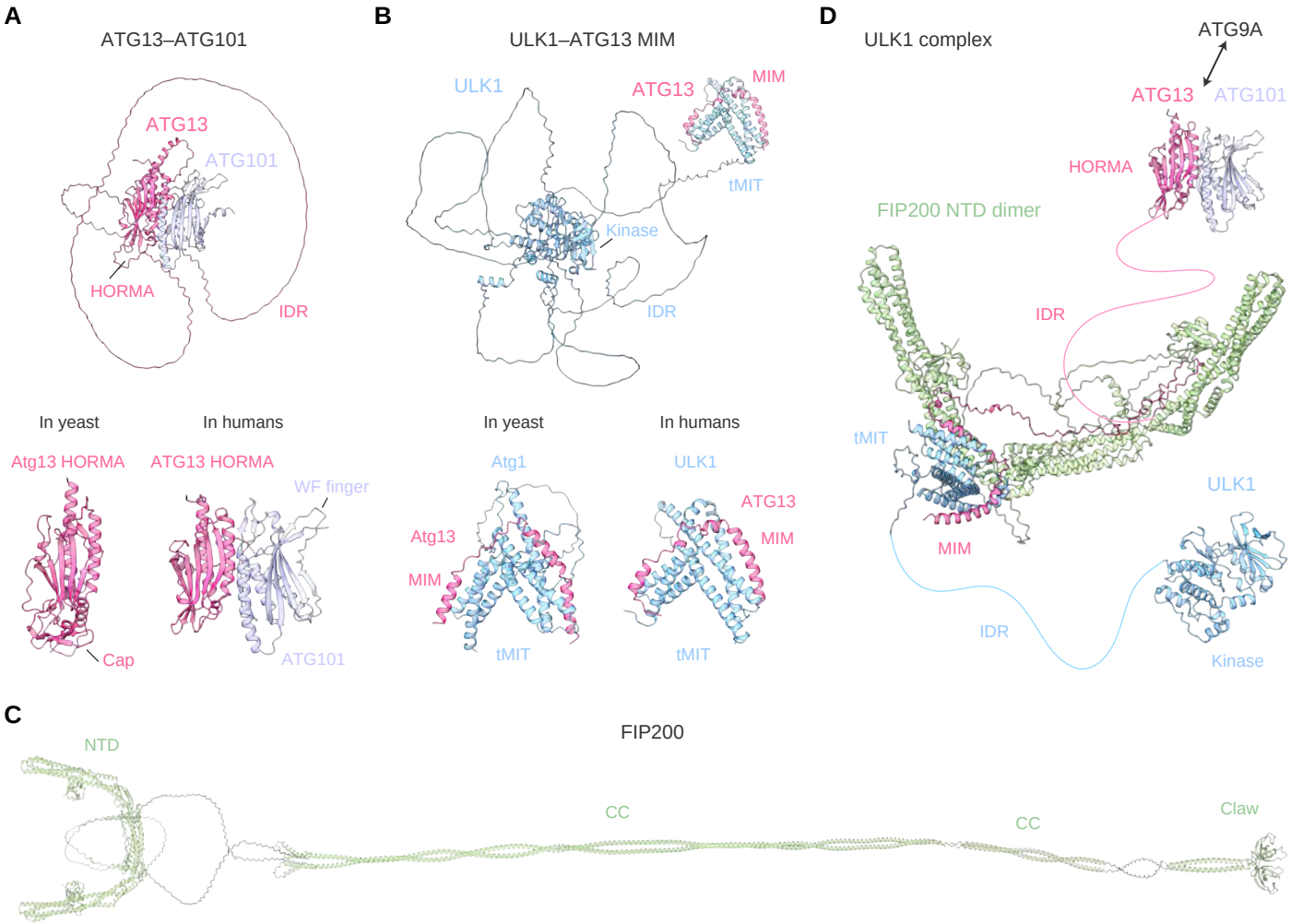

A
ATG13–ATG101
ATG13
ATG101
HORMA
IDR
In yeast
In humans
Atg13 HORMA
ATG13 HORMA
WF finger
Cap
ATG101
B
ULK1–ATG13 MIM
ULK1
ATG13
MIM
tMIT
Kinase
IDR
In yeast
In humans
Atg1
Atg13
MIM
tMIT
ULK1
ATG13
MIM
tMIT
D
ULK1 complex
ATG9A
ATG13
ATG101
HORMA
FIP200 NTD dimer
IDR
tMIT
MIM
ULK1
IDR
Kinase
C
FIP200
NTD
CC
CC
Claw

Figure 4

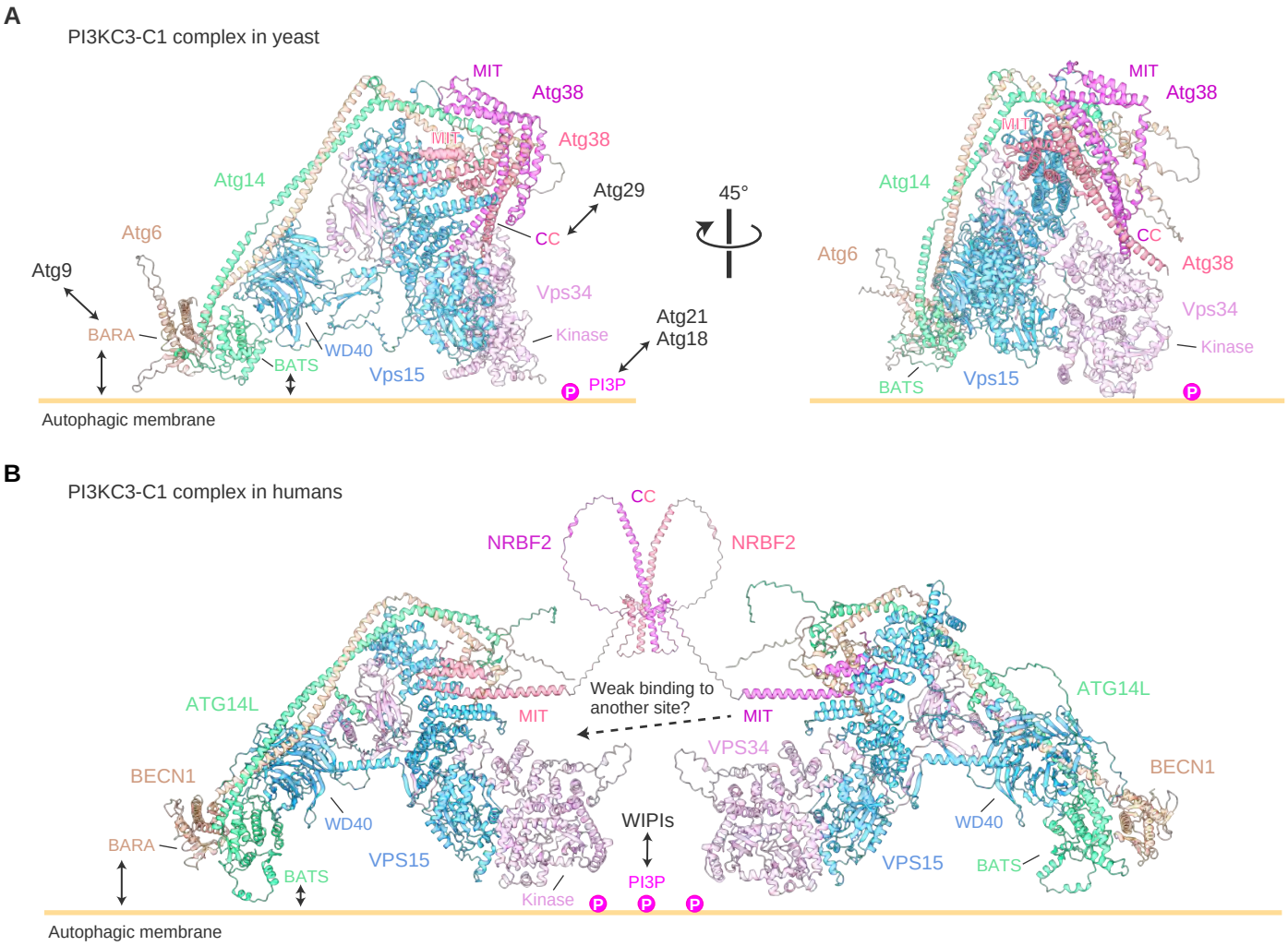

A
PI3KC3-C1 complex in yeast
MIT
Atg38
MIT
Atg38
Atg14
Atg29
45°
Atg6
CC
Atg9
Vps34
BARA
Kinase
Atg21
Atg18
WD40
BATS
Vps15
PI3P
Autophagic membrane
MIT
Atg38
MIT
Atg14
CC
Atg6
Atg38
Vps34
Kinase
BATS
Vps15
B
PI3KC3-C1 complex in humans
CC
NRBF2
NRBF2
ATG14L
Weak binding to
another site?
MIT
MIT
ATG14L
VPS34
BECN1
BECN1
WD40
WIPIs
WD40
BARA
VPS15
BATS
PI3P
VPS15
BATS
Kinase
Autophagic membrane

Figure 5

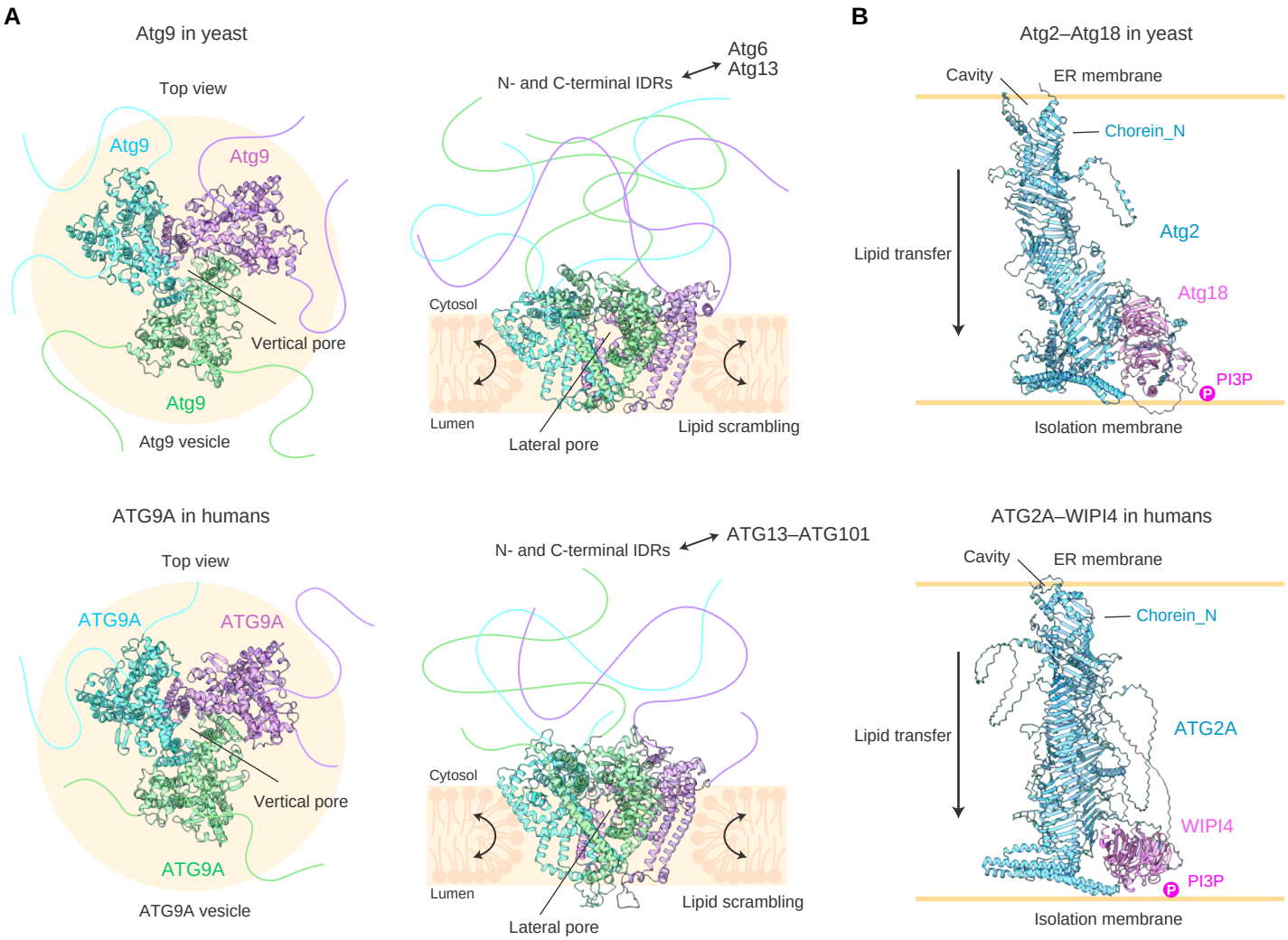
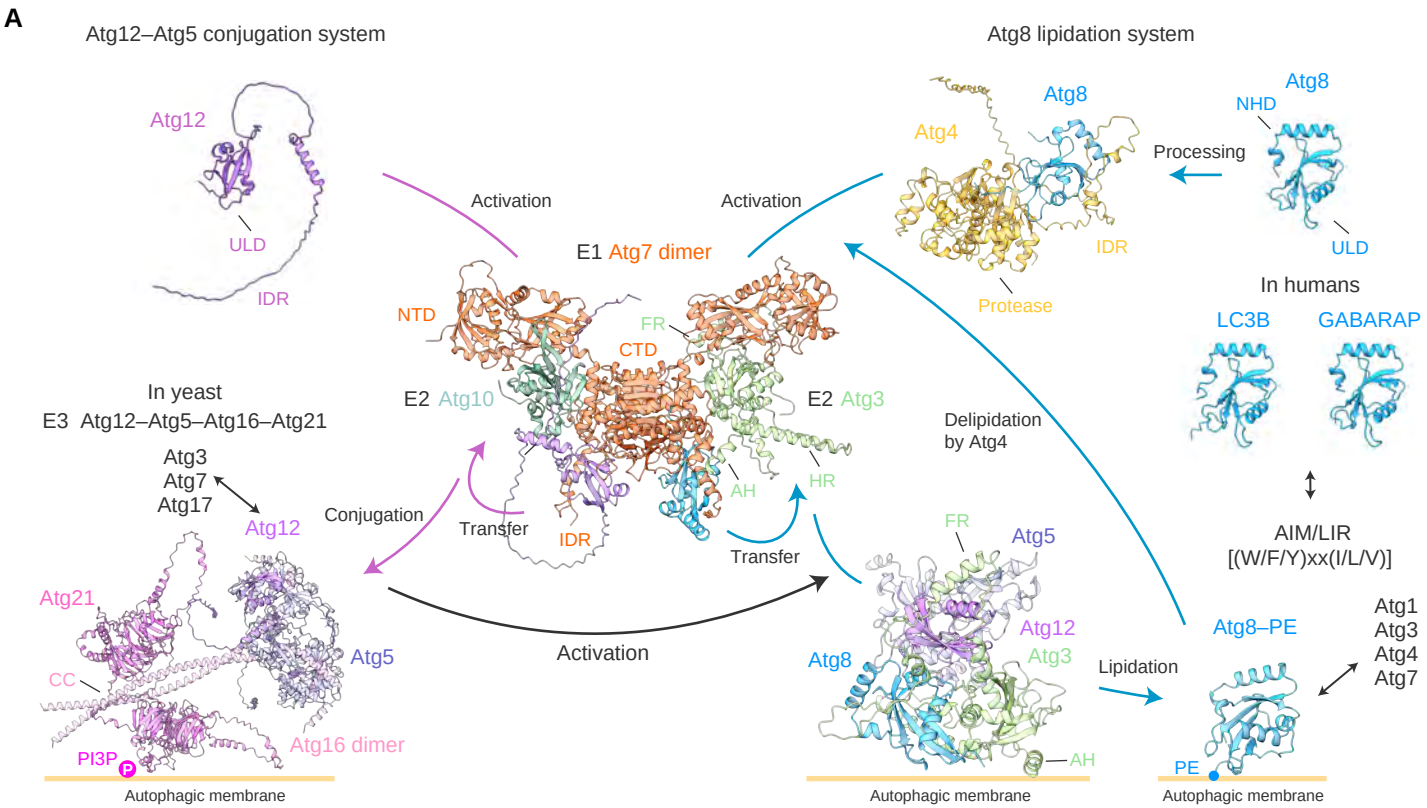

A
Atg9 in yeast
Top view
Atg9
Atg9
Vertical pore
Atg9
Atg9 vesicle
Atg6
Atg13
N- and C-terminal IDRs
Cytosol
Lumen
Lateral pore
Lipid scrambling
ATG9A in humans
Top view
ATG9A
ATG9A
Vertical pore
ATG9A
ATG9A vesicle
ATG13–ATG101
N- and C-terminal IDRs
Cytosol
Lumen
Lateral pore
Lipid scrambling
B
Atg2–Atg18 in yeast
Cavity
ER membrane
Chorein_N
Lipid transfer
Atg2
Atg18
PI3P
Isolation membrane
ATG2A–WIPI4 in humans
Cavity
ER membrane
Chorein_N
Lipid transfer
ATG2A
WIPI4
PI3P
Isolation membrane

Figure 6


A
Atg12–Atg5 conjugation system
Atg8 lipidation system
Atg12
ULD
IDR
Activation
Activation
E1 Atg7 dimer
NTD
FR
CTD
E2 Atg10
E2 Atg3
AH
HR
IDR
Transfer
Transfer
Conjugation
In yeast
E3 Atg12–Atg5–Atg16–Atg21
Atg3
Atg7
Atg17
Atg12
Atg21
Atg5
CC
PI3P
Atg16 dimer
Autophagic membrane
Activation
Atg8
Atg4
IDR
Protease
Processing
Atg8
NHD
ULD
In humans
LC3B
GABARAP
Delipidation
by Atg4
AIM/LIR
[(W/F/Y)xx(I/L/V)]
FR
Atg5
Atg12
Atg3
Atg8
AH
Autophagic membrane
Lipidation
Atg8–PE
PE
Atg1
Atg3
Atg4
Atg7
Autophagic membrane
B
In humans
E3 ATG12–ATG5–ATG16L1–WIPI2
ATG3
ATG12
ATG5
WIPI2
WD40
WIPI2
CC
ATG16L1 dimer
PI3P
Autophagic membrane
C
Autophagic membrane scaffold
E1
Atg7
E2
Atg3
E3
Atg12–Atg5–Atg16
NTD
FR
HR
AH
IDR
Atg8–PE
CC
PE
Autophagic membrane